

# Nonholonomic billiards and bounded motion in cylinders

Christopher Cox\*, Renato Feres† Zijie Hu†

February 16, 2026

## Abstract

A widely used mathematical model for the bouncing motion of an ideally elastic ball—referred to in previous work by the first two authors and collaborators as a *no-slip billiard* system—exhibits some notable dynamical behavior that is not well-understood. For example, under certain initial conditions, the axial component of the position of the center of the ball moving inside a vertical solid cylinder under constant gravitational force does not accelerate downward as might be expected but remains bounded. There is not as yet, as far as we know, any analytical study of the bouncing ball dynamics, under gravity, in general cylinders (not necessarily having a circular cross-section) in  $\mathbb{R}^3$ . In this paper, we propose an approach by comparing the no-slip system with a smooth approximation of it that we call *nonholonomic billiards*. It consists of a 4-dimensional ball rolling on the solid 3-dimensional cylinder. We first review earlier work on no-slip billiards and their connection with nonholonomic (rolling) systems, explain how nonholonomic billiards approximate the no-slip kind (after work by the first two authors and B. Zhao), and illustrate the relationship with a few numerical case studies that demonstrate the utility of the soft (nonholonomic) system as a helpful tool for exploring the dynamics of no-slip billiard systems.

## 1 INTRODUCTION

The following geometric-mechanical problem is one of the motivations for the present paper. A perfectly elastic ball is thrown against the inner surface of a cylindrical wall. The subsequent motion is under the influence of constant gravitational force directed downward along the cylinder axis. The ball then undergoes a sequence of bounces, with parabolic (falling) motion in between. We imagine the surface of the rigid, spherical ball as ideally rubbery, which causes the contact with the wall’s inner surface to be perfectly nonslippery, in a sense to be shortly defined. This no-slip property imposes at each collision a coupling of the ball’s rotational and linear momentum. The cylinder need not have circular cross-section; it encloses a region  $\mathcal{R} = \mathcal{C} \times \mathbb{R} \subseteq \mathbb{R}^3$ , where  $\mathcal{C} \subseteq \mathbb{R}^2$ . For

---

\*Department of Mathematics and Statistics, University of Massachusetts Amherst, 710 N. Pleasant Street, Amherst, MA 01003

†Department of Mathematics, Washington University, Campus Box 1146, St. Louis, MO 63130

example, when  $\mathcal{C}$  is a strip in  $\mathbb{R}^2$  bounded by two parallel lines,  $\mathcal{R}$  is the region between two parallel, vertical walls.

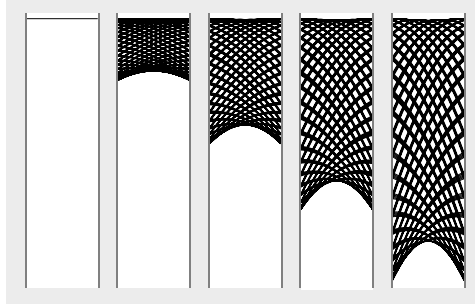


Figure 1: No-slip disc bouncing between two parallel vertical lines, under gravity, with increasing values of the acceleration-due-to-gravity parameter  $g$  increasing from left to right. On the far left,  $g = 0$  and the trajectory is periodic of period 2.

The question we ask is then: what can be said about the ball's vertical motion? In particular, can the motion remain bounded so that the ball does not fall below a certain height? In this section we review a few pertinent results from a couple of papers by the first two authors together with B. Zhao [3], and T. Chumley and S. Cook [4]. It turns out that trajectories of the no-slip billiard system under gravity are bounded in the case of parallel vertical walls (in any dimension); see Figure 1, which shows trajectories of the center of the ball in dimension 2 under increasing values of the acceleration due to gravity.

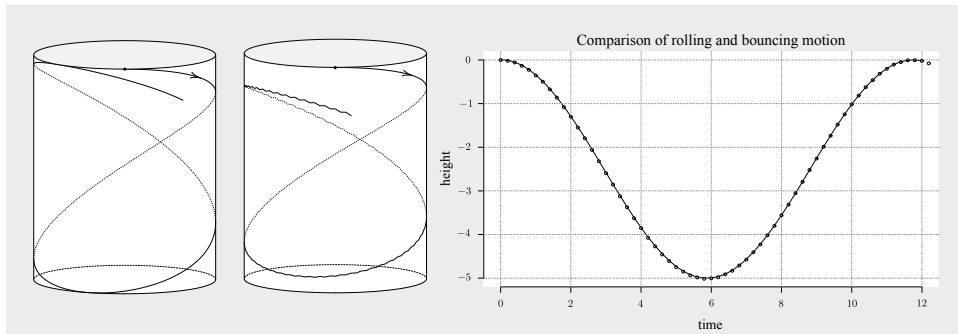


Figure 2: Left: segment of trajectory of the center of a ball rolling on the inner surface of a cylinder, under gravity, showing harmonic vertical motion. Center: trajectory of a no-slip billiard ball, with very short bouncing steps, not satisfying the initial rolling impact assumption. Right: under that assumption, the no-slip billiard ball closely tracks the rolling motion.

The motion is also bounded in 3-dimensional circular cylinders under a natural assumption on initial conditions that we call *rolling impact*. This case is particularly interesting

as it highlights the similarities with the classical and well-known mechanical system consisting of a ball rolling without slipping on the inner wall of a cylinder, under gravity, for which the vertical component of the motion oscillates harmonically. See [4] and the left image in the below Figure 2. The initial condition on the linear and angular velocities ensuring bounded motion is this: the velocity of the point on the ball in contact with the cylindrical surface at the time of first collision should have zero component along the tangent line to the circular cross section. In other words, this initial velocity (which, we stress, is not the center velocity but the velocity of a boundary point on the ball) should lie in the vertical plane containing the cylinder axis and the point of contact. We say in this case that the initial (linear and angular) velocities satisfy a *rolling impact* condition.

The vertical component of the center of the ball bouncing inside the circular cylinder is shown as a function of time by the graph on the right-hand side of Figure 2. There it is assumed that the first collision satisfies rolling impact. This generates a sequence of closely spaced bounces (think of a skipping stone) that precisely tracks the rolling motion.

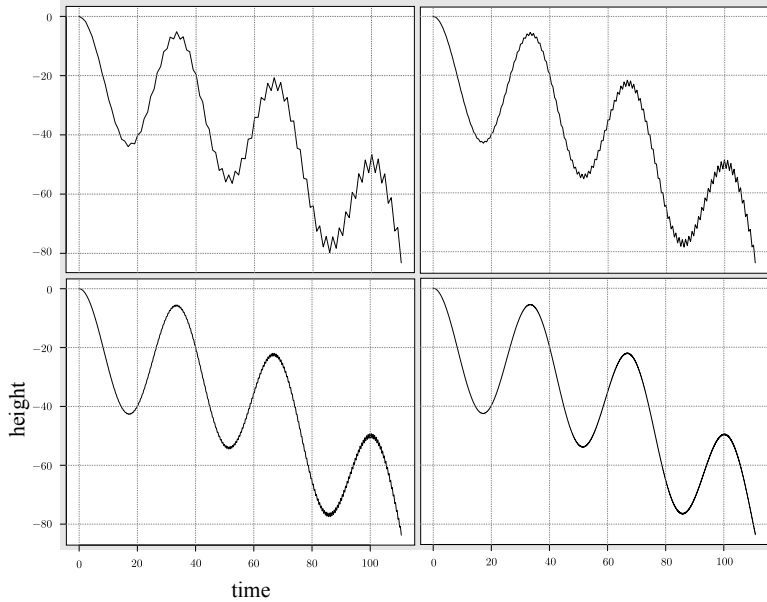


Figure 3: Height of the ball's center as a function of time when the rolling first impact assumption is not satisfied. The sequence of graphs (NW → NE → SW → SE) was generated with decreasing lengths of the skipping motion steps. An apparent energy dissipation into the zig-zag motion at smaller and smaller scales produces accelerated falling and decreasing amplitude of oscillation.

Boundedness of trajectories was noted in the two dimensional strip with gravity in [10] and then later proved rigorously for more general cases in [4], but neither argument is as illuminating as may be wished. For example, the proof does not relate the bouncing motion to rolling and so does not explain why the former can so closely shadow the latter as shown in Figure 2. In particular, one can expect the skipping motion illustrated by the

graph of Figure 2 to converge to a solution to the rolling differential equations (to be given later). Obtaining this limit is so far, to us, a challenging problem. Part of the subtlety is already apparent in the middle image of Figure 2. When the rolling impact condition is not satisfied, the bouncing motion with short bouncing steps exhibits a zig-zag small scale component that increases in amplitude with time. In the limit of bouncing steps approaching 0, it is natural to conjecture that some sort of rolling trajectory is obtained which, however, incorporates energy dissipation through this infinitesimal zig-zag motion, causing the ball’s descent to accelerate and the amplitude of oscillation to decrease, as illustrated in Figure 3. Obtaining the equations for such dissipative rolling motion is an interesting problem that is not addressed here.

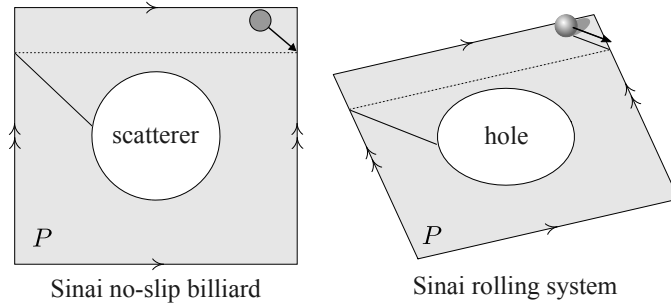


Figure 4: Left: a two-dimensional no-slip billiard system on a Sinai billiard table. Right: the associated 3-dimensional rolling system. With appropriately adjusted moment of inertia parameters for the disc and the ball, the rolling-around-the-edge of the circular hole, on the right, converges to the no-slip billiard reflection off the circular scatterer, on the left, as the radius of the ball approaches 0. This suggests that the two systems have comparable dynamical properties, and that the rolling system, governed by differential equations, can help us to understand the other—impact driven—system. The one on the left may be regarded as the two-dimensional shadow of that on the right, while the one on the right defines a soft-collisions version of the other.

A promising approach to a detailed analysis of these no-slip billiard systems is suggested by [3], which establishes a much more direct connection between no-slip billiards and nonholonomic systems. Stated somewhat vaguely for now, a no-slip billiard system in an  $n$ -dimensional submanifold  $\mathcal{R} \subseteq \mathbb{R}^n$  with boundary can be approximated, for small values of the ball radius, by the rolling of an  $n + 1$ -dimensional ball on  $\mathcal{R} \subseteq \mathbb{R}^{n+1}$ , with appropriately set moment of inertia parameter. See Figure 4. (Away from the boundary edges and in the absence of gravity, the motion of the center of the rolling ball is uniform and rectilinear.) In this way, the study of a billiard-like system driven by discrete impulsive forces can, in principle, be approached via the analysis of a nonholonomic system governed by differential equations, at the cost of passing from dimension  $n$  to dimension  $n + 1$ . We call the latter class of systems *nonholonomic billiards*. This term has been previously used in [1], which was the inspiration for [3]. In the former paper, however, it has a different definition in a much more restricted setting. The two types of nonholonomic billiards are, nevertheless, sufficiently close conceptually that using the

same name seems to us appropriate.

Our main goal in this paper, in addition to reviewing a few of the results mentioned above, is to explore, by a combination of analytic and numerical methods, some examples of such nonholonomic billiard systems in cylinders under gravity and indicate the similarities with their no-slip counterparts.

## 2 NO-SLIP BILLIARD SYSTEMS

### 2.1 GENERALITIES

A few definitions are needed to make precise the above description of the *no-slip* bouncing ball, referred to here as a *no-slip billiard system*. Let the ball of radius  $r$  centered at the origin of  $\mathbb{R}^n$  be  $B := B_0(r)$  and define a mass distribution on  $B$  by a rotationally invariant finite Borel measure  $\mu$  on  $B$  of total mass  $m$ . The mass-normalized matrix  $L = (\ell_{ij})$  of second moments of  $\mu$  is defined by

$$\ell_{ij} := \frac{1}{m} \int_B x_i x_j \, d\mu(x),$$

where  $x = (x_1, \dots, x_n)$  are the standard Cartesian coordinates in  $\mathbb{R}^n$ . Rotational symmetry implies that  $L$  is a scalar matrix,  $L = \lambda I$ , where  $I$  is the identity matrix in dimension  $n$ . It will be useful to express the moment of inertia parameter  $\lambda$  in a couple of different forms. We first define the dimensionless parameter

$$\gamma := \sqrt{2\lambda}/r.$$

For example,  $\gamma = \sqrt{\frac{2}{n+2}}$  for a uniform mass distribution in dimension  $n$ . Let  $\mathcal{R}_0$  be a region in  $\mathbb{R}^n$  and define the *billiard domain*  $\mathcal{R}$  as the closure of the set of  $x \in \mathbb{R}^n$  for which the open ball  $B_x(r)$  of center  $x$  and radius  $r$  is contained in  $\mathcal{R}_0$ . We assume that  $\mathcal{R}_0$  is sufficiently regular and  $r$  sufficiently small that  $\mathcal{R}$  has piecewise smooth boundary, possibly with corners. On a regular point  $a$  on the boundary of  $\mathcal{R}$  (that is, a point at which the tangent space to the boundary of  $\mathcal{R}$  exists) define the unit normal vector  $\nu(a) = \nu_a$  pointing towards the interior of  $\mathcal{R}$ . Denote by  $SE(n)$  the special Euclidean group of positive isometries of  $\mathbb{R}^n$ , whose elements are pairs  $(A, a) \in SO(n) \times \mathbb{R}^n$  representing the affine transformation  $x \mapsto Ax + a$ . The configuration manifold of the ball-in- $\mathcal{R}_0$  system is  $M \subseteq SE(n)$  consisting of all  $(A, a) \in SE(n)$  such that  $a \in \mathcal{R}$ . Thus  $M$  is a submanifold of  $SE(n)$  with boundary and possibly corners, trivially fibered over  $\mathcal{R}$ , with typical fiber given by the rotation group  $SO(n)$ . Elements in the Lie algebra of  $SE(n)$  will be written  $(U, u)$  where  $U \in \mathfrak{so}(n)$ —the *angular velocity*—is a skew-symmetric  $n \times n$  matrix and  $u \in \mathbb{R}^n$  is the velocity of the center of the ball.

From the mass distribution measure  $\mu$  we obtain the kinetic energy Riemannian metric in  $M$  as follows. Tangent vectors  $\xi, \eta$  in  $T_q M$  at configuration  $q = (A, a)$  may be written as  $\xi = (U_\xi A, u_\xi)$  with  $(U_\xi, u_\xi) \in \mathfrak{so}(n) \times \mathbb{R}^n$ . The kinetic energy of the system in configuration  $q$  and kinetic state  $\xi$  is obtained by integrating over  $B$  the kinetic energy

$$\frac{1}{2} |V_\xi(x)|^2 \, d\mu(x)$$

of a mass element  $d\mu(x)$ , where  $V_\xi(x) \in \mathbb{R}^n$  is the velocity vector of the material point  $x$  in the kinetic state  $\xi$ . The inner product on  $T_q M$  associated to the kinetic energy quadratic form is easily obtained:

$$\langle \xi, \zeta \rangle_q := m \left\{ \frac{(r\gamma)^2}{2} \text{Tr} \left( U_\xi U_\zeta^\top \right) + u_\xi \cdot u_\zeta \right\}.$$

The tangent bundle to the boundary of  $M$  contains a vector subbundle  $\mathfrak{R}$ , which we call the *rolling* subbundle, needed for the definition of the no-slip condition. At a regular boundary point  $q = (A, a)$  of  $M$  (so that  $a$  lies in the regular boundary of  $\mathcal{R}$ ) the rolling subspace of  $T_q M$  is

$$\mathfrak{R}_q := \{(UA, u) \in T_q M : u = rU\nu_a\}.$$

Note that the point on the boundary of the ball in contact with the boundary of  $\mathcal{R}_0$  at a collision configuration has zero velocity in the kinetic state  $(UA, u) \in \mathfrak{R}_q$ . This is implied by the equation  $u = rU\nu_a$ .

## 2.2 THE NO-SLIP COLLISION MAP

The ball's kinetic state immediately after a collision,  $C_q \xi$ , is a function of the state  $\xi$  immediately before. This *collision map*  $C_q : T_q M \rightarrow T_q M$  is assumed to have the following properties: (1) it is a linear, (2) preserves kinetic energy, (3) satisfies time reversibility, (4) it restricts to the identity on the rolling space  $\mathfrak{R}_q$ . This last assumption is justified by noting that, at the moment of collision, the point on the moving ball in contact with the boundary of  $\mathcal{R}_0$  has zero velocity for a kinetic state in  $\mathfrak{R}_q$ , and thus no change in linear or angular momentum should occur. Such  $\xi \in \mathfrak{R}_q$  physically corresponds to a rolling and grazing collision. We refer to [7], by the first two authors, for more details on the classification of such collision maps. It is interesting to observe, as noted in [7], that condition (4) follows from the physically natural requirement that impulse forces causing the ball to bounce off the wall hypersurface must act only upon the point of contact. (In principle, one may conceive of more general impulse force fields with an extended range of action, such as would happen when shape deformation during a collision event is also modeled.) These four assumptions characterize  $C_q$  as an orthogonal linear involution that restricts to the identity map on the rolling subspace.

If we further assume isotropic ball surface properties (effectively, the map  $C_q = C_a$  does not depend on  $A$ ), then it is not difficult to conclude (see [7]) that there are only two possibilities for  $C_q$ , determined by whether this map's restriction to  $\mathfrak{R}_q^\perp$ —the orthogonal complement to the rolling subspace—is the identity or its negative: in the first case, which we call *slippery* or *standard* collision map (the term *smooth* is widely used in the physics and engineering literature), the velocity of the center of the ball reflects specularly and angular momentum is unchanged; ignoring angular momentum and tracking the motion by the position of the ball's center, one obtains ordinary billiard dynamics. The second possibility, for which  $C_q|_{\mathfrak{R}_q^\perp}$  is the negative of the identity map, corresponds to what we call *no-slip* collision.

The explicit form of  $C_q = C_a$  acting on  $\xi = (UA, u) \cong (U, u) \in \mathfrak{se}(n)$  (the latter being

the Lie algebra of  $SE(n)$ ) is

$$(1) \quad C_a(U, u) = \left( U + \frac{s_\beta}{\gamma r} \nu_a \wedge [u - rU\nu_a], c_\beta u - \frac{s_\beta}{\gamma} (u \cdot \nu_a) \nu_a + s_\beta \gamma r U \nu_a \right),$$

where

$$c_\beta := \cos \beta := \frac{1 - \gamma^2}{1 + \gamma^2}, \quad s_\beta := \sin \beta := \frac{2\gamma}{1 + \gamma^2},$$

$u \cdot v$  is the ordinary dot product, and  $\wedge : \mathbb{R}^n \times \mathbb{R}^n \rightarrow \mathfrak{so}(n)$  is the generalized cross product of vectors: if  $u, v \in \mathbb{R}^n$  then  $u \wedge v$  is the skew-symmetric matrix such that

$$(u \wedge v)w := (u \cdot w)v - (v \cdot w)u.$$

The no-slip assumption is typically used as model for energy preserving impacts involving rigid spherical bodies when coupling of linear and angular momentum is expected at collisions. Examples are given in [2, 5, 6, 8, 9, 11, 12].

A more revealing form of Equation (1) is obtained with the following minor change in notation. Let  $V_a$  be the tangent space to the boundary of  $\mathcal{R}$  at a regular boundary point  $a$  and denote by  $\Pi_a$  the orthogonal projection from  $\mathbb{R}^n$  to  $V_a$ . Then

$$T_a \mathcal{R} = V_a \oplus R\nu_a$$

and, as shown in [3], any  $U \in \mathfrak{so}(n)$  has the decomposition

$$U = \Pi_a U \Pi_a + \nu_a \wedge U \nu_a,$$

where  $\Pi_a U \Pi_a \in \mathfrak{so}(V_a)$  is an infinitesimal rotation on  $V_a := T_a(\partial \mathcal{R})$ . Now define

$$\bar{u} := \Pi_a u, \quad S := \gamma r U, \quad \bar{S} := \Pi_a S \Pi_a, \quad W := W_S := S \nu_a.$$

Both  $\bar{u}$  and  $W$  are tangent vectors in  $V_a$ . Let us use the same symbol  $C_a$  to represent the collision map in the new variables  $(S, u)$ . Then Equation (1) becomes

$$(2) \quad C_a(S, u) = (\bar{S}, 0) + (0, -u \cdot \nu_a \nu_a) + (\nu_a \wedge (s_\beta \bar{u} - c_\beta W), c_\beta \bar{u} + s_\beta W).$$

Separating components, note that

$$(3) \quad \bar{S} \mapsto \bar{S}, \quad \nu_a \mapsto -\nu_a, \quad \begin{pmatrix} \bar{u} \\ W \end{pmatrix} \mapsto \begin{pmatrix} c_\beta & s_\beta \\ s_\beta & -c_\beta \end{pmatrix} \begin{pmatrix} \bar{u} \\ W \end{pmatrix}.$$

For simplicity, we have omitted the  $(n-1) \times (n-1)$  identity matrix (more precisely, the identity map on  $V_a$ ) multiplying each  $s_\beta, c_\beta$  in the above block matrix. Since  $c_\beta^2 + s_\beta^2 = 1$ , the map

$$\begin{pmatrix} \bar{u} \\ W \end{pmatrix} \mapsto \begin{pmatrix} c_\beta & s_\beta \\ s_\beta & -c_\beta \end{pmatrix} \begin{pmatrix} \bar{u} \\ W \end{pmatrix} = \begin{pmatrix} c_\beta & -s_\beta \\ s_\beta & c_\beta \end{pmatrix} \begin{pmatrix} \bar{u} \\ -W \end{pmatrix}$$

is, as expected, an orthogonal transformation with negative determinant. The identity on the right shows that the transformation amounts to a sign change of  $W$  composed

with a rotation by the characteristic angle  $\beta$  (a parameter serving as proxy for the moment of inertia) that mixes up (and thus couples) linear velocity and certain components of the angular velocity matrix. When the moment of inertia parameter  $\gamma$  is zero, the characteristic angle  $\beta$  is also zero and the block matrix reduces to the identity. In this case,

$$\begin{pmatrix} \bar{u} \\ W \end{pmatrix} \mapsto \begin{pmatrix} \bar{u} \\ -W \end{pmatrix},$$

so that  $\bar{u}$  and  $W$  are fully decoupled. Later we will return to this collision map and compare it with a rolling-over-the-edge map for nonholonomic billiards. A manifestation of time reversibility is the involutive property

$$\begin{pmatrix} c_\beta & s_\beta \\ s_\beta & -c_\beta \end{pmatrix}^2 = I.$$

It is useful to register here that, using the  $\bar{S}$  and  $W$  definitions, the kinetic energy Riemannian metric takes the form

$$(4) \quad \langle \xi, \zeta \rangle_q := m \left\{ \frac{1}{2} \text{Tr} \left( \bar{S}_\xi \bar{S}_\zeta^\top \right) + W_\xi \cdot W_\zeta + u_\xi \cdot u_\zeta \right\}.$$

### 2.3 DIMENSIONS 2 AND 3

For two-dimensional regions ( $n = 2$ ),  $\bar{S} = 0$  and the inner product (4) reduces to standard dot product in  $\mathbb{R}^3$ , in which the third variable is (the one-dimensional)  $W$ . In this case,  $S = sJ$ , where  $J$  is positive (counterclockwise) rotation by  $\pi/2$  in  $\mathbb{R}^2$  and at a boundary point  $a$  of the planar billiard region  $\mathcal{R}$ , we have  $W = S\nu = s\tau_a$ , where  $\tau$  is the unit tangent vector to the boundary curve of  $\mathcal{R}$  oriented counterclockwise.

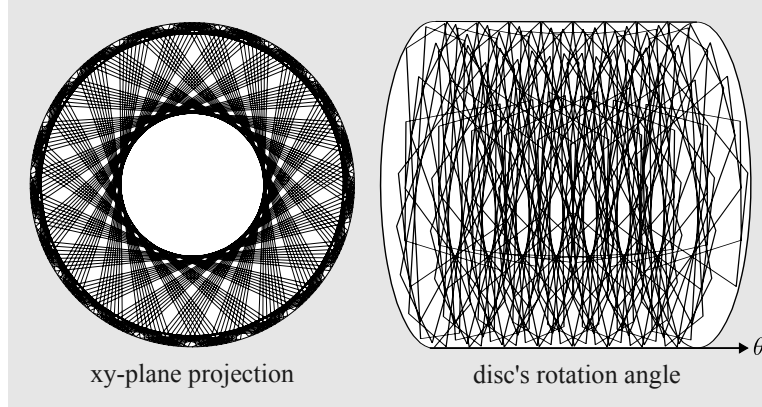


Figure 5: Trajectory of a no-slip billiard system on a disc. Left: trajectory of the moving disc's center, showing the characteristic double caustic. Right: 3-dimensional configuration space trajectory, including the moving disc's rotation angle.

The kinetic state of the billiard disc is specified by  $(\hat{u}, \bar{u}, s)$ , where  $\hat{u} = u \cdot \nu_a$  and  $\bar{u} = u \cdot \tau_a$ , and the collision map becomes

$$C_a : \begin{pmatrix} \hat{u} \\ \bar{u} \\ s \end{pmatrix} \mapsto \begin{pmatrix} -1 & 0 & 0 \\ 0 & c_\beta & s_\beta \\ 0 & s_\beta & -c_\beta \end{pmatrix} \begin{pmatrix} \hat{u} \\ \bar{u} \\ s \end{pmatrix}.$$

Figure 5 shows a segment of trajectory of a no-slip billiard system on a disc shaped table. The actual trajectory is in the 3-dimensional solid torus  $D \times S^1$ , where the disc  $D$  contains the positions of the center of the moving particle (also a disc) and  $S^1$  the orientations in space. (The figure shows an orbit segment in the covering space  $D \times \mathbb{R}$  rather than  $D \times S^1$ .) The projection of the center of the moving disc to the circular table (left of Figure 5) shows a characteristic double caustic, an easy to understand feature based solely on time reversibility and symmetry of the billiard domain. When the moment of inertia is 0 ( $\gamma = 0$ ), one obtains an ordinary billiard trajectory with a single caustic circle.

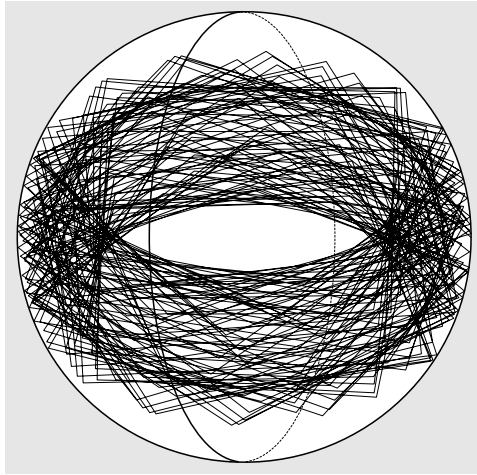


Figure 6: A segment of trajectory of the center of a no-slip ball in a sphere.

For  $n = 3$ , let  $J_a$  be the operator of positive rotation by  $\pi/2$  on the 2-dimensional  $V_a$  (the tangent space to the boundary of  $\mathcal{R}$  at  $a$ .) Here *positive* is defined by the outward pointing  $\nu_a$  (and the right-hand rule of vector calculus.) Then  $\bar{S} = \bar{s}J_a$ ,  $\bar{s} \in \mathbb{R}$  may be called the *tangential spin* at the point of contact with the boundary. In this case,  $(\bar{s}, W)$  may be used as proxies for  $S$  and

$$\langle \xi, \zeta \rangle_q := m(\bar{s}_\xi \bar{s}_\zeta + W_\xi \cdot W_\zeta + u_\xi \cdot u_\zeta),$$

while the no-slip collision map takes the form

$$C_a : \begin{pmatrix} \bar{s} \\ \hat{u} \\ \bar{u} \\ W \end{pmatrix} \mapsto \begin{pmatrix} 1 & 0 & 0 & 0 \\ 0 & -1 & 0 & 0 \\ 0 & 0 & c_\beta & s_\beta \\ 0 & 0 & s_\beta & -c_\beta \end{pmatrix} \begin{pmatrix} \bar{s} \\ \hat{u} \\ \bar{u} \\ W \end{pmatrix}.$$

This is a linear map in  $SO(6)$ . As before,  $\hat{u} := u \cdot \nu_a$ . The invariance of  $\bar{s}$  makes physical sense: a change in  $\bar{s}$  would require an infinite impulsive torque tangent to the wall, acting on the ball at the single point of contact. It is also not surprising that the normal component of the linear velocity changes sign. The essence of the no-slip collision map lies in the coupling of linear and angular velocities controlled by the parameter  $\gamma$  that defines  $c_\beta, s_\beta$ .

As an example, Figure 6 shows a segment of trajectory of the center of a no-slip ball bouncing inside a sphere. The figure shows a characteristic spherical annulus containing the trajectory. It is not clear how to explain all the (numerically) observed features of this example based on symmetry considerations. For example, it is an interesting exercise to determine the axis and width of this annular envelope as a function of a trajectory's initial conditions.

## 2.4 NO-SLIP BILLIARDS IN GENERAL CYLINDERS

Let  $\mathcal{R} = \overline{\mathcal{R}} \times \mathbb{R}$  be an  $(n+1)$ -dimensional domain with  $\overline{\mathcal{R}} \subseteq \mathbb{R}^n$  a billiard domain in dimension  $n$ . We call such region a *cylinder*. We refer to  $e := (0, \dots, 0, 1)$  as the *cylinder axis* unit vector and to  $\overline{\mathcal{R}}$  as the *cross-section*. Let  $\nu$  be the outward pointing unit normal vector field on the boundary of  $\mathcal{R}$ , which is also a unit normal vector field on the boundary of  $\overline{\mathcal{R}}$ . It turns out that the orthogonal projection of trajectories of the no-slip billiard ball in  $\mathcal{R}$  to the cross-section are trajectories of the no-slip  $n$ -dimensional (projected) ball on  $\overline{\mathcal{R}}$ . The two balls in different dimensions are assumed to have the same moment of inertia parameter  $\gamma$  or  $\beta$ .

**Theorem 1.** *Let  $\Pi$  be the orthogonal projection from  $\mathbb{R}^{n+1}$  to  $\mathbb{R}^n$ . Then  $\Pi$  maps trajectories of the no-slip billiard system in a cylinder of dimension  $n+1$  to trajectories of the corresponding cross-sectional no-slip billiard system in dimension  $n$ , assuming the moment of inertia parameters of the two systems are the same. This holds even when the  $(n+1)$ -dimensional ball is subjected to a constant force parallel to the axis of the cylinder.*

Before proving Theorem 1, we need a few definitions. At any regular  $a$  on the boundary of  $\mathcal{R}$ , let  $\Pi_{\nu_a}^\perp$  be the orthogonal projection to the hyperplane  $\nu_a^\perp$ ,  $\Pi_e^\perp$  be the orthogonal projection to the hyperplane  $e^\perp$ , and  $\Pi_a$  be the orthogonal projection to the codimension-2 subspace  $(\text{span}\{\nu_a, e\})^\perp$ . Let  $\mathfrak{se}(e_a^\perp)$  be the Lie algebra of the Euclidean group on the hyperplane orthogonal to  $e$  at  $a$  and  $\mathfrak{se}(n)$  be the Lie algebra of the Euclidean group on  $\mathbb{R}^n \cong \mathbb{R}^n \times \{0\}$ , regarded as the subspace of  $\mathbb{R}^{n+1}$ . These two Lie algebras are naturally isomorphic.

Theorem 1 is now a corollary of the following three propositions.

**Proposition 2.** *Define the  $(n+1)$ -dimensional space*

$$(5) \quad (e \wedge e_a^\perp, \mathbb{R}e) := \{(e \wedge v, \lambda e) \in \mathfrak{se}(n+1) : v \cdot e = 0 \text{ and } \lambda \in \mathbb{R}\}.$$

*Then*

$$\mathfrak{se}(n+1) = \mathfrak{se}(e_a^\perp) \oplus (e \wedge e^\perp, \mathbb{R}e)$$

*is an orthogonal direct sum of vector spaces. (The second summand is not a Lie algebra.)*

*Proof.* Orthogonality relative to the inner product

$$\langle (S_1, u_1), (S_2, u_2) \rangle := m \left\{ \frac{1}{2} \text{Tr} (S_1 S_2^\top) + u_1 \cdot u_2 \right\}$$

is readily checked. Equality then follows from counting dimensions:

$$\frac{(n+1)(n+2)}{2} = \frac{n(n+1)}{2} + n + 1$$

and  $\dim \mathfrak{se}(n) = \frac{n(n+1)}{2}$ .  $\square$

**Proposition 3.** *The no-slip collision map  $C_a$  respects the orthogonal decomposition (5).*

*Proof.* Since  $C_a$  is orthogonal, it suffices to show that  $C_a$  maps  $(e \wedge e^\perp, \mathbb{R}e)$  to itself. Now

$$C_a(e \wedge v, \lambda e) = (e \wedge v', \lambda' e)$$

where

$$v' = \Pi_a v - (s_\beta \lambda + c_\beta \nu_a \cdot v) \nu_a, \quad \lambda' = c_\beta \lambda - s_\beta \nu_a \cdot v.$$

This is obtained from a direct application of  $C_a$  in the form of Equation (2).  $\square$

**Proposition 4.** *The projection map  $\Pi_e^\perp$  intertwines the collision map  $C_a$  on  $\mathfrak{se}(n+1)$  associated to the no-slip billiard system on  $\mathcal{R}$  and the collision map  $C_{\bar{a}}$  on  $\mathfrak{se}(n)$  associated to the no-slip billiard system on  $\bar{\mathcal{R}}$ , where  $\bar{a} := \Pi_e^\perp a$ . Both maps  $C_a$  and  $C_{\bar{a}}$  are assumed to have the same moment of inertia parameter  $\gamma$  (or  $\beta$ ).*

*Proof.* We can verify that  $\Pi_e^\perp \circ C_a = C_{\bar{a}} \circ \Pi_e^\perp$  holds by a straightforward application of the explicit form of the collision maps as given in Equation (2). One should keep in mind that  $\Pi_e^\perp$  maps  $(S, u)$  to  $(\Pi_e^\perp S \Pi_e^\perp, \Pi_e^\perp u)$ .  $\square$

Note that an external force cannot affect the discontinuous change in velocities at a collision event. Physically, impact forces are very intense over a very short time interval, during which ordinary forces will have negligible contribution to changing the particle's linear and angular momentum. Additionally, a force parallel to the axis of the cylinder will not affect the projection of trajectories to cross-sectional hyperplanes.

## 2.5 A REMARK CONCERNING SYMMETRIES

It is useful to note that Euclidean isometries (not necessarily orientation preserving) mapping the boundary of  $\mathcal{R}$  to itself are symmetries of the no-slip system in the sense of the following proposition. Notations are as follows. Suppose  $f \in E(n)$  is an Euclidean isometry (not necessarily positive) mapping the regular boundary point  $a$  in  $\mathcal{R}$  to another such point  $f(a)$  for which  $F_a \nu_a = \nu_{f(a)}$ , where  $F_a := df_a$  is the differential of  $f$  at  $a$ . It follows that  $F_a$  maps  $V_a$  to  $V_{f(a)}$  (recall that  $V_a$  denotes the tangent space at  $a$  to the boundary of  $\mathcal{R}$ .) It is easily checked that

$$F_a \Pi_a = \Pi_{f(a)} F_a, \quad F_a \bar{u} = \overline{F_a u}, \quad F_a (u \wedge v) F_a^{-1} = F_a u \wedge F_a v, \quad F_a W_S = W_{F_a S F_a^{-1}}.$$

Writing, for simplicity,  $f_a u := F_a u$  and  $f_a S := F_a S F_a^{-1}$ , we obtain the transformations

$$\bar{u} \mapsto f_a \bar{u} = \overline{f_a u}, \quad \bar{S} \mapsto f_a \bar{S} = \overline{f_a S}, \quad W_S \mapsto f_a W = W_{f_a S}, \quad (\bar{u}, W) \mapsto (f_a \bar{u}, f_a W).$$

From these and (3) we obtain the equivariant property of the collision map:

$$f_a \circ C_a = C_{f(a)} \circ f_a.$$

This holds, in particular, whenever the Euclidean isometry  $f \in E(n)$  restricts to a self-map of (the boundary of)  $\mathcal{R}$ . We say in this case that  $f$  is a *symmetry* of the no-slip billiard system. Let us write the action of  $f$  on the no-slip billiard map as  $f^* C$ , so that

$$(f^* C)_a := f_a^{-1} \circ C_{f(a)} \circ f_a.$$

Then  $f$  is a symmetry of the no-slip billiard system if  $f^* C = C$ . We conclude:

**Proposition 5.** *Any Euclidean isometry mapping  $\mathcal{R}$  to itself is a symmetry of the no-slip billiard system.*

### 3 ROLLING SYSTEMS

Rolling systems are classical examples of nonholonomic mechanical systems. An especially convenient set of equations describing the motion motion of a rigid sphere with rotationally symmetric mass distribution rolling on submanifolds of Euclidean space (of arbitrary codimension) was obtained in [3] and is reviewed in this section. These equations show, in particular, that such systems may be regarded as one-parameter deformations of geodesic flows on hypersurfaces in  $\mathbb{R}^{n+1}$ , with moment of inertia serving as the deformation parameter.

#### 3.1 PRELIMINARIES

By a *rolling system* we mean a dynamical system of geometric/mechanical nature consisting of the following elements: a submanifold  $P$  of  $\mathbb{R}^{n+1}$  possibly with boundary and corners, and arbitrary codimension; an  $(n+1)$ -dimensional ball of radius  $r$  which rolls over  $P$  without slipping—according to definition to be given shortly—and may roll over the edge upon reaching the boundary of  $P$ . We suppose the ball has rotationally symmetric mass distribution with the moment of inertia parameter  $\gamma$  defined in our discussion of no-slip billiard systems. We further suppose  $r$  to be sufficiently small, and the boundary of  $P$  regular enough, that the boundary  $\mathcal{N} = \mathcal{N}_r$  of the tubular neighborhood of  $P$ —the set of points in  $\mathbb{R}^{n+1}$  at a distance less than or equal to  $r$  from  $P$ —is a piecewise smooth, everywhere differentiable hypersurface. In other words, the unit normal vector field  $\nu$  to  $\mathcal{N}$ , pointing away from  $P$ , is everywhere continuous and piecewise smooth. Thus it is possible that the principal curvatures of  $\mathcal{N}$  will have jump discontinuities near the boundary of  $P$ . (See Figure 7.) Figure 8 shows the rolling over the (single point) edge where  $P$  is the (codimension-2) half-infinite line in  $\mathbb{R}^3$ .

The configuration manifold of the rolling ball is the product  $SO(n+1) \times \mathcal{N} \subseteq SE(n+1)$ . A point  $(A, a)$  in this space represents the Euclidean motion mapping the ball of radius

$r$  centered at  $0 \in \mathbb{R}^{n+1}$  to the ball centered at  $a \in \mathcal{N}$  under the function  $x \mapsto Ax + a$ . Due to rotational symmetry, we only need the position of the ball's center  $a \in \mathcal{N}$  at each moment in time in order to specify its configuration. The ball's kinetic state is given by the velocity  $v \in T_a \mathcal{N}$  of the ball's center and the angular velocity  $U \in \mathfrak{so}(n+1)$ . The condition of no-slip rolling is

$$(6) \quad v = rU\nu(a).$$

This is the nonholonomic constraint on the ball's motion asserting that the point on the surface of the ball in contact with  $P$  has zero velocity.

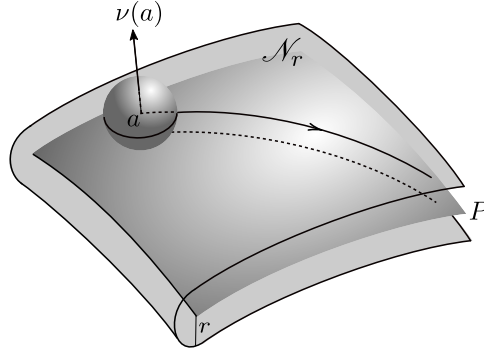


Figure 7:  $P$  is a smooth submanifold of  $\mathbb{R}^{n+1}$  possibly with boundary and corners, and arbitrary codimension, on which a ball of radius  $r$  can roll. The locus of centers of the rolling ball is the hypersurface  $\mathcal{N} = \mathcal{N}_r$ , which is the boundary of an  $r$ -tubular neighborhood of  $P$ . The unit normal vector field to  $\mathcal{N}$  is denoted  $\nu$ .

As was done for the no-slip billiard ball, we prefer to work not with the actual angular velocity matrix  $U$ , whose entries have physical dimension [1/time], but with the matrix  $r\gamma U$ , whose entries have physical dimension [velocity]. We define

$$S := r\gamma \Pi_a U \Pi_a \in \mathfrak{so}(T_a \mathcal{N}),$$

where  $\Pi_a$  is the orthogonal projection from  $\mathbb{R}^{n+1}$  to  $T_a \mathcal{N}$  and  $\mathfrak{so}(T_a \mathcal{N})$  is the Lie algebra of skew-symmetric linear maps from  $T_a \mathcal{N}$  to itself relative to the standard (dot product) Riemannian metric on  $\mathcal{N}$ . It turns out that the kinetic state of the rolling ball is fully specified by  $a$  (for the configuration),  $S$  and  $v$ . In fact, it is not difficult to show (see [3]) that

$$U = \Pi_a U \Pi_a + \nu_a \wedge U \nu_a$$

which, together with the constraint equation (6), gives

$$r\gamma U = S + \gamma \nu_a \wedge v.$$

We call  $S$  the *tangential spin* of the rolling ball. Thus it is natural to look for the equations of motion on a vector bundle  $\mathcal{M}$  over  $\mathcal{N}$  that extends the tangent bundle  $T\mathcal{N}$

by incorporating the tangential spin. We define

$$(7) \quad \pi : \mathcal{M} := \mathfrak{so}(\mathcal{N}) \oplus T\mathcal{N} \rightarrow \mathcal{N},$$

whose fiber over  $a \in \mathcal{N}$  is  $\mathfrak{so}(T_a\mathcal{N}) \oplus T_a\mathcal{N}$ . Sections of  $\mathcal{M}$  consist of pairs  $(S, X)$  where  $X$  is a vector field on  $\mathcal{N}$  and  $S$  is a field of skew-symmetric endomorphisms on tangent spaces of  $\mathcal{N}$ . There is on  $\mathcal{M}$  a bundle Riemannian metric

$$(8) \quad \langle \xi, \zeta \rangle_a = m \left\{ \frac{1}{2} \text{Tr} (S_\xi S_\zeta^\top) + v_\xi \cdot v_\zeta \right\},$$

which is naturally associated to the moving ball's kinetic energy:

$$E_a(\xi) = \frac{1}{2} \|\xi\|^2 := \frac{1}{2} m \left\{ \frac{1}{2} \text{Tr} (SS^\top) + |v|^2 \right\},$$

for a state  $\xi = (S, v)$  at  $a$ . Note that the direct sum in (7) is orthogonal.

When  $n = 2$ ,  $\mathfrak{so}(\mathcal{N})$  is a trivial line bundle with global section defined at each  $a$  by the map, denoted  $J_a$ , that performs counterclockwise rotation by  $\pi/2$  on  $T_a\mathcal{N}$ . In this case,  $\mathcal{M} \cong \mathbb{R} \times T\mathcal{N}$  and the tangential spin reduces to a scalar quantity  $s$ .

### 3.2 A CONNECTION ON $\mathcal{M}$

Elements of the Euclidean group  $SE(n+1)$  have been written as pairs  $(A, a)$ , acting on points  $x \in B_r(0)$  (the ball of radius  $r$  centered at the origin) by affine transformations  $x \mapsto Ax + a$ . Thus it was natural to also use  $a$  to designate points in  $\mathcal{N}$ . From now on, as the group and its Lie algebra take a back seat and we focus attention on  $\mathcal{N}$ , points on this manifold will, typically, be indicated by  $x$ .

We now introduce a connection on  $\mathcal{M}$  as follows. Recall the  $\wedge$  product (generalizing the cross-product of vector calculus)

$$\wedge : T_x\mathcal{N} \times T_x\mathcal{N} \rightarrow \mathfrak{so}(T_x\mathcal{N}).$$

The Riemannian metric induced on  $\mathcal{N}$  by restriction of the dot product in Euclidean space will, when convenient, be written as  $\langle X, Y \rangle_x$  rather than  $X(x) \cdot Y(x)$ .

**Proposition 6.** *The Levi-Civita connection on  $T\mathcal{N}$  naturally induces a connection  $\nabla$  on  $\mathcal{M}$ . This connection is metric relative to the Riemannian metric (8) and satisfies the product rule*

$$(9) \quad \nabla_u X \wedge Y = (\nabla_u X) \wedge Y + X \wedge \nabla_u Y,$$

where  $X, Y$  are smooth vector fields on  $\mathcal{N}$ .

*Proof.* The Levi-Civita connection  $\nabla$  naturally extends from vector to general tensor fields on  $\mathcal{N}$  and, in particular, to fields of endomorphisms, or  $(1, 1)$ -tensor fields. Under this extension,  $\nabla$  satisfies the product rule with respect to tensor product and the pairing between vectors and covectors. Thus the product rule (9) holds since

$$X \wedge Y = Y \otimes X^\flat - X \otimes Y^\flat,$$

where  $X^\flat := \langle X, \cdot \rangle$  is the covector field associated to  $X$  via the Riemannian matrix on  $\mathcal{N}$ . Proving that  $\nabla$  is Riemannian on  $\mathcal{M}$  only requires checking that

$$X\text{Tr}(S_1 S_2) = \text{Tr}((\nabla_X S_1) S_2) + \text{Tr}(S_1 (\nabla_X S_2)).$$

(The transpose has been dropped since  $S^\top = -S$ .) This can be verified as follows. Let  $E_1, \dots, E_n$  be a local orthonormal frame of vector fields on  $\mathcal{N}$ . Then

$$\text{Tr}(S_1 S_2) = \sum_j \langle E_j, S_1 S_2 E_j \rangle = - \sum_j \langle S_1 E_j, S_2 E_j \rangle.$$

Now  $S_i E_j$  is a local vector field on  $\mathcal{N}$  and (from general properties of the covariant derivative on general tensor fields, in particular the product rule for contractions)

$$\nabla_X (S_i E_j) = (\nabla_X S_i) E_j + S_i (\nabla_X E_j).$$

This implies

$$\begin{aligned} -X \langle S_1 E_j, S_2 E_j \rangle &= \langle S_2 (\nabla_X S_1) E_j, E_j \rangle + \langle S_1 (\nabla_X S_2) E_j, E_j \rangle \\ &\quad + \langle S_1 \nabla_X E_j, S_2 E_j \rangle + \langle S_1 E_j, S_2 \nabla_X E_j \rangle. \end{aligned}$$

Summing over  $j$ ,

$$\begin{aligned} X\text{Tr}(S_1 S_2) &= \text{Tr}((\nabla_X S_1) S_2) + \text{Tr}(S_1 (\nabla_X S_2)) \\ &\quad + \sum_j (\langle S_1 \nabla_X E_j, S_2 E_j \rangle + \langle S_1 E_j, S_2 \nabla_X E_j \rangle). \end{aligned}$$

It remains to show that the sum in the previous identity vanishes. Substituting

$$\nabla_X E_j = \sum_k \langle E_k, \nabla_X E_j \rangle E_k$$

into that sum (indicated by  $\mathcal{I}$ ) results in

$$\mathcal{I} = \sum_{j,k} \langle E_k, \nabla_X E_j \rangle (\langle S_1 E_k, S_2 E_j \rangle + \langle S_1 E_j, S_2 E_k \rangle).$$

But it is now apparent that  $\mathcal{I}$  is the trace of the product of a skew-symmetric matrix and a symmetric matrix, which is 0.  $\square$

### 3.3 THE FREE ROLLING EQUATIONS

The *shape operator* of the hypersurface  $\mathcal{N}$  is defined at each  $x \in \mathcal{N}$  by the symmetric linear map

$$\mathbb{S}_x : u \in T_x \mathcal{N} \mapsto \mathbb{S}_x u := -D_u \nu \in T_x \mathcal{N},$$

in which  $D_u \nu$  is the directional derivative of the unit normal vector field  $\nu$  in the direction of  $u \in T_x \mathcal{N}$ . The eigenvectors of  $\mathbb{S}_x$  are the *principal directions* at  $x$ , and the associated eigenvalues are the *principal curvatures* of  $\mathcal{N}$  at  $x$ .

We can now describe the equations of motion for a ball with rotationally symmetric mass distribution and moment of inertia parameter  $\gamma$  in a form that does not require explicit use of the nonholonomic constraint equation. It will be convenient to introduce yet another proxy for the moment of inertia:

$$(10) \quad \eta := \frac{\gamma}{\sqrt{1 + \gamma^2}}.$$

The following theorem is from [3].

**Theorem 7.** *The motion of a rolling ball of radius  $r$  on the submanifold  $P \subseteq \mathbb{R}^{n+1}$  with moment of inertia parameter  $\eta$  is given by a curve  $x(t) \in \mathcal{N}_r$  and a differentiable section  $(S(t), v(t))$  of  $\mathcal{M}$  such that  $v(t) = x'(t)$  and*

$$\frac{\nabla v}{dt} = -\eta S \mathbb{S}_x v, \quad \frac{\nabla S}{dt} = \eta (\mathbb{S}_x v) \wedge v.$$

Let us make a few observations about this set of equations.

1. When the moment of inertia parameter  $\eta$  is zero, the two equations decouple and the system reduces to

$$\frac{\nabla x'}{dt} = 0, \quad \frac{\nabla S}{dt} = 0.$$

This means that the trajectories of the center of the rolling ball are geodesics in  $\mathcal{N}$  and the tangential spin  $S(t)$  is a parallel tensor field along those geodesics. This is reminiscent of frame flows on Riemannian manifolds, except that it is not a frame but some kind of frame spinning that undergoes parallel transport. Thus we can regard the above rolling equations as a one-parameter deformation of (a bundle extension of) the geodesic flow on the tangent bundle of  $\mathcal{N}$ . See Figure 8.

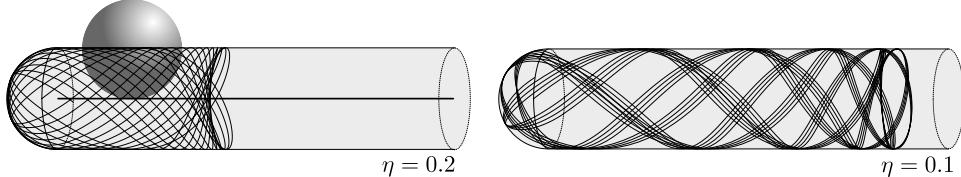


Figure 8: A 3-dimensional ball rolling without slipping on a half-infinite line  $P$  in  $\mathbb{R}^3$ , showing the rolling at the boundary of  $P$ . As the moment of inertia parameter  $\eta$  is reduced, trajectories approach geodesics on the boundary  $\mathcal{N}_r$  of the  $r$ -tubular neighborhood of  $P$ .

2. The dynamical properties of the system depend strongly on the extrinsic curvatures of  $\mathcal{N}$  via the shape operator. When  $\mathbb{S} = 0$ , the center of the rolling ball follows uniform rectilinear motion (on the flat  $\mathcal{N}$ ) while  $S(t)$  is parallel; hence the components of  $S(t)$  are conserved quantities.

3. Let us define the bundle map  $f : \mathcal{M}_x \rightarrow \mathcal{M}_x$  at each  $x \in \mathcal{N}$  (in which  $\mathcal{M}_x$  indicates the fiber of  $\mathcal{M}$  over  $x$ ) by

$$f(S, v) = ((\mathbb{S}_x v) \wedge v, -S\mathbb{S}_x v).$$

Then the rolling equations may be written as

$$\frac{\nabla \xi}{dt} = \eta f(\xi).$$

It is an easy exercise to check that  $\langle \xi, f(\xi) \rangle = 0$ , from which it follows that

$$\frac{d}{dt} E(\xi(t)) = \frac{1}{2} \frac{d}{dt} \langle \xi(t), \xi(t) \rangle = \left\langle \xi(t), \frac{\nabla \xi}{dt}(t) \right\rangle = \langle \xi(t), f(\xi(t)) \rangle = 0.$$

This shows conservation of energy for the rolling equation.

4. It is not difficult to verify that the rolling equations are time-reversible.

5. The vector bundle  $\mathcal{M}$  can be identified with the tangent bundle of a Riemannian manifold  $M$ , as follows. Let  $\pi : M \rightarrow \mathcal{N}$  be the fiber bundle of linear isometries on tangent spaces of  $\mathcal{N}$ . By definition, the fiber  $M_x$  over  $x \in \mathcal{N}$  consists of all the orientation preserving linear maps  $A : T_x \mathcal{N} \rightarrow T_x \mathcal{N}$  such that  $\langle Au, Av \rangle_x = \langle u, v \rangle_x$  for all  $x \in \mathcal{N}$  and all  $u, v \in T_x \mathcal{N}$ . In other words,  $M$  is a bundle of groups, the fiber over  $x$  being the special orthogonal group on the inner product vector space  $(T_x \mathcal{N}, \langle \cdot, \cdot \rangle_x)$ . We denote this group by  $SO(\mathcal{N})_x$  and its Lie algebra by  $\mathfrak{so}(\mathcal{N})_x$ . The tangent bundle of  $M$  can be identified with  $\mathcal{M}$  as follows. Let  $e \in TM$  have base-point  $A \in M$ , where  $A \in SO(\mathcal{N})_x$ . Let  $t \mapsto A(t) \in M$  be a differentiable curve representing  $e$  in the sense that  $A(0) = A$  and  $A'(0) = e$ . We can then map  $e$  to the pair  $(S, u)$  where

$$u = \left. \frac{d}{dt} \right|_{t=0} \pi(A(t)) \in T_x \mathcal{N}, \quad S = r\gamma \left( \left. \frac{\nabla}{dt} \right|_{t=0} A(t) \right) A^{-1} \in \mathfrak{so}(\mathcal{N})_x.$$

Here  $\nabla$  is the covariant derivative obtained through the imbedding  $M \subseteq T\mathcal{N} \otimes T^*\mathcal{N}$ . Through the identification  $TM \cong \mathcal{M}$ , the manifold  $M$  acquires a Riemannian metric and a metric connection  $\nabla$ . It is natural to ask whether  $\nabla$  is the Levi-Civita connection on  $M$ , which amounts to determining whether the torsion tensor of  $\nabla$  vanishes. This is a question we have not yet addressed.

### 3.4 ROLLING UNDER EXTERNAL FORCES

We briefly remark on how external forces can be incorporated into the rolling equations of Theorem 7. Let  $\varphi x$  be a force (per unit mass) vector field on  $\mathbb{R}^{n+1}$ . This means that  $\varphi(Ax + a)d\mu(x)$  is the force vector acting on an element of mass  $d\mu(x)$  of the ball in configuration  $g = (A, a)$ , where  $x$  is here a point on the ball  $B_r(0)$  of radius  $r$  centered at the origin. We obtain a linear functional on the tangent space at  $g$  to the configuration manifold  $SO(n+1) \times \mathcal{N}$  of the rolling ball:

$$\hat{\varphi}_g(\xi) := \int_{B_r(0)} V_\xi(x) \cdot \varphi(Ax + a) d\mu(x).$$

Recall that  $V_\xi(x) \in \mathbb{R}^{n+1}$  denotes the velocity of the material point  $x \in B_r(0)$  in configuration  $g$  and kinetic state  $\xi \in T_g(SO(n+1) \times \mathcal{N})$ . We call  $\hat{\varphi}$  the *power functional*. Under the assumption that  $\mu$  is rotationally symmetric, we obtain (using the trace inner product and notations from Section 2.1)

$$\hat{\varphi}_g(\xi) = \langle (U_\xi, u_\xi), (\Psi(a), \psi(a)) \rangle_g,$$

where

$$\Psi(a) := \frac{1}{(r\gamma)^2} \int_{B_r(0)} x \wedge \varphi(x+a) \frac{d\mu(x)}{m}, \quad \psi(a) := \int_{B_r(0)} \varphi(x+a) \frac{d\mu(x)}{m}.$$

Going through the argument from [3] used to derive the free equations of motion of Theorem 7, but now taking account of the external forces, which affect the determination of the rolling constraint force, one obtains (after switching once again the roles of  $a$  and  $x$ ; see the beginning of Section 3.2) the equations

$$(11) \quad \frac{\nabla v}{dt} = -\eta S \mathbb{S}_x v + r\eta^2 \Psi \nu + \frac{1}{1+\gamma^2} \Pi_x \psi, \quad \frac{\nabla S}{dt} = \eta (\mathbb{S}_x v) \wedge v + r\eta \Pi_x \Psi \Pi_x.$$

Here  $\Pi = \Pi_x$  is the orthogonal projection map to  $T_x \mathcal{N}$ . Of interest in this paper is the case of a constant  $\varphi$ , for which  $\Psi = 0$  and  $\psi = \varphi$ .

## 4 NO-SLIP BILLIARDS AS LIMITS OF ROLLING SYSTEMS

We can finally indicate the connection between no-slip billiards and rolling systems. The key remark is based on determining the outcome of rolling around a straight edge. Thus suppose that  $P$  is the (codimension-1) half-space  $\mathbb{R}^{n-1} \times [0, \infty)$  in  $\mathbb{R}^{n+1}$ , the boundary of which is  $\mathbb{R}^{n-1}$ . Rolling around the edge then corresponds to the rolling of an  $(n+1)$ -dimensional ball on  $\mathbb{R}^{n-1}$ . The curved part of the hypersurface  $\mathcal{N}_r$  is part of the boundary of the tubular neighborhood of  $\partial P$ , which is  $\mathbb{R}^{n-1} \times S^1(r)$ , where  $S^1(r)$  is the circle of radius  $r$  on the plane perpendicular to  $\mathbb{R}^{n-1}$  in  $\mathbb{R}^{n+1}$ . See Figure 9.

In order to solve the rolling equations in this setting (Theorem 7), it is convenient to express  $v$  and  $S$  in the parallel orthonormal frame described in Figure 9. Thus we write

$$v = \sum_i v_i E_i, \quad S = \frac{1}{2} \sum_{i,j} S_{ji} E_i \wedge E_j, \quad S_{ji} := E_i \cdot (S E_j).$$

Since the  $\nabla_v E_i$  are parallel and  $\mathbb{S}_x E_i = -\frac{1}{r} \delta_{ni} E_i$  (on the curved part of  $\mathcal{N}$ ), we have

$$\frac{\nabla v}{dt} = \sum_i \dot{v}_i E_i = -\eta S \mathbb{S}_x v = \frac{\eta v_n}{r} S E_n,$$

where  $\dot{v}_i$  is derivative in the time variable. Taking the inner product with  $E_i$  gives

$$\dot{v}_n = 0, \quad \dot{v}_i = \frac{\eta v_n}{r} S_{ni} \text{ for } i < n.$$

Note that  $v_n$  is constant because  $S_{nn} = 0$ . Similarly, (as the  $E_i$  are parallel)

$$\dot{S}_{ij} = E_i \cdot \left( \frac{\nabla S}{dt} E_j \right) = \eta E_i \cdot ((\mathbb{S}_x v) \wedge v E_j) = -\frac{\eta}{r} E_i \cdot (E_n \wedge v E_j) = -\frac{\eta}{r} (\delta_{nj} v_i - \delta_{ni} v_j).$$

Thus we are left with the elementary problem of solving the system

$$\dot{v}_n = 0, \quad \dot{S}_{ij} = 0 \text{ for } i, j < n, \quad \dot{S}_{ni} = -\frac{\eta v_n}{r} v_i \text{ and } \dot{v}_i = \frac{\eta v_n}{r} S_{ni} \text{ for } i < n.$$

Let us solve for the velocities immediately after leaving the round edge as a function of the velocities immediately before entering it.

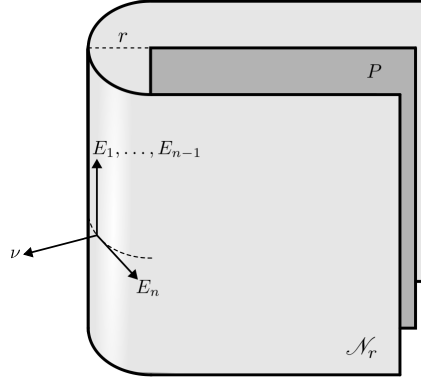


Figure 9: The unit vector fields  $E_1, \dots, E_n$  form a parallel orthonormal frame on  $\mathcal{N}$  consisting of principal directions.  $E_n$  is associated to principal curvature  $-1/r$  whereas the principal curvatures for the other vectors are 0.

We define

$$\bar{v} := \sum_{i=1}^{n-1} (E_i \cdot v) E_i, \quad W := S E_n.$$

Note that both  $\bar{v}$  and  $W$  lie in  $\mathbb{R}^{n-1}$ . These are the velocity components that do not remain constant in the process of rounding the edge of the flat plate  $P$ . The time it takes to go around the edge is  $T = \pi r/v_n$ . Integrating from 0 to  $T$  the system

$$\frac{d}{dt} \begin{pmatrix} \bar{v} \\ W \end{pmatrix} = \frac{\eta\pi}{T} \begin{pmatrix} 0 & I \\ -I & 0 \end{pmatrix} \begin{pmatrix} \bar{v} \\ W \end{pmatrix}$$

gives

$$(12) \quad \begin{pmatrix} \bar{v}(T) \\ W(T) \end{pmatrix} = \begin{pmatrix} \cos(\pi\eta)I & -\sin(\pi\eta)I \\ \sin(\pi\eta)I & \cos(\pi\eta)I \end{pmatrix} \begin{pmatrix} \bar{v}(0) \\ W(0) \end{pmatrix}.$$

Let us now change our perspective somewhat and imagine looking at the folded hypersurface of Figure 9 from above and seeing its two sheets connected by the half-cylinder

as one. From this perspective, the rolling around the edge is perceived as a soft collision with a flat wall. We rewrite the transformation of Equation (12) accordingly, as follows. The vector field  $E_n$  is viewed as pointing out on the edge ( $\cong \mathbb{R}^{n-1}$ ) of the lower flat part of  $\mathcal{N}$ , and pointing in at the edge of the upper flat part. If we now identify both edges and replace  $E_n$  there with the unit outward pointing normal vector field  $\mathbf{n}$ , redefine  $W$  as  $S\mathbf{n}$ , and introduce  $\hat{v} := v \cdot \mathbf{n}$ , the transformation (12) becomes

$$\begin{pmatrix} \hat{v} \\ \bar{v} \\ W \end{pmatrix} \mapsto \begin{pmatrix} -1 & 0 & 0 \\ 0 & \cos(\pi\eta)I & \sin(\pi\eta)I \\ 0 & \sin(\pi\eta)I & -\cos(\pi\eta)I \end{pmatrix} \begin{pmatrix} \hat{v} \\ \bar{v} \\ W \end{pmatrix}.$$

This expression should be compared with the corresponding map for the no-slip billiard collision, Equation (3). They become identical if we equate the two moment of inertia parameters  $\beta = \pi\eta$ . Returning to the more basic parameter  $\gamma$ , and writing  $\gamma_n$  and  $\gamma_{n+1}$  for those parameters in dimensions  $n$  and  $n+1$ , we have

$$(13) \quad \frac{1 - \gamma_n^2}{1 + \gamma_n^2} = \cos \left( \frac{\gamma_{n+1}}{\sqrt{1 + \gamma_{n+1}^2}} \pi \right).$$

When  $r$  is very small, so that the time the ball spends in contact with the edge of  $P$  can be neglected, and if the moment of inertia parameters are related as indicated above, then the rolling-around-the-edge map in dimension  $n+1$  becomes indistinguishable from the no-slip collision map for the no-slip billiard system in dimension  $n$ . If the edge of  $P$  is curved, the determination of the outgoing velocities away from the edge of  $P$  as a function of the incoming velocities will be much more difficult, as will be seen in later examples. But it can be expected that, as the radius of the ball approaches 0, the principal curvatures of the edge of  $P$  as perceived by the rolling ball become negligible, and the flat approximation can be used. This is the key idea behind the proof of the following theorem from [3].

**Theorem 8** ([3]). *Let  $P$  be a domain in  $\mathbb{R}^n \cong \mathbb{R}^n \times \{0\} \subseteq \mathbb{R}^{n+1}$  with smooth boundary  $P_0$  whose principal curvatures (as a hypersurface in  $P$ ) are uniformly bounded. Consider an  $(n+1)$ -dimensional ball with spherically symmetric mass distribution constrained to roll without slip on  $P$ . We assume no forces other than those enforcing the constraint. In the limit when the radius of the ball approaches 0, solutions of the rolling ball equation have the following description: On  $P \setminus P_0$  the point-mass moves with constant velocities  $v$  and  $S$  (this is also true for positive radius); upon reaching a boundary point  $x \in P_0$  with unit normal vector  $\mathbf{n}(x)$ , the vector  $(v, W) \in T_x P \oplus T_x P_0$ , with  $W = S\mathbf{n}(x)$ , undergoes a reflection according to the no-slip collision map  $C_x$  as described in Equation (2). The moment of inertia parameters  $\gamma_{\text{no-slip}}$  (going into  $C_x$ ) and  $\gamma_{\text{roll}}$  (defining  $\eta$  in the rolling equations), both independent of the ball radius, are related to each other by Equation (13).*

In the presence of external forces, the segments of trajectories on the flat part of  $P$  will, naturally, no longer follow a uniform rectilinear motion, but such forces do not affect what happens at the boundary in the limit  $r \rightarrow 0$ .

**Definition 9** (Nonholonomic billiard system). *By a nonholonomic billiard system we mean a rolling system on a flat plate  $P$  as in Theorem 8, for a ball with positive radius, rotationally symmetric mass distribution, with or without external forces.*

We may think of nonholonomic billiard systems as soft versions of no-slip billiards.

#### 4.1 ROLLING ON VERTICAL STRIPS UNDER GRAVITY

We are now in a position to begin addressing the main point of this paper, which is to use the nonholonomic billiards, governed by systems of ordinary differential equations, as a tool to help illuminate and explain some of the observed behavior of no-slip billiards, in particular the bounded trajectories on cylinders under gravity. This is a project we only begin here; it will be systematically developed elsewhere. In this section, we consider the case of a no-slip disc bouncing between two parallel vertical lines (Figure 1).

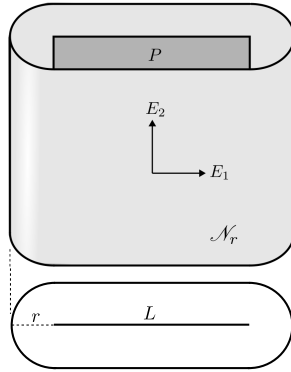


Figure 10: Segment of the cylindrical surface  $\mathcal{N}_r$  associated to an infinite vertical flat strip  $P$  in  $\mathbb{R}^3$ . Constant acceleration due to gravity is  $-gE_2$ , where  $E_1, E_2$  form a parallel orthonormal frame on  $\mathcal{N}_r$ .

The following fact, from [4], lends support to the above expressed hope for the usefulness of the nonholonomic billiards. It deals with rolling in vertical cylinders in dimension 3 under constant gravity.

**Theorem 10** ([4]). *Suppose the cross-section of the 3-dimensional vertical cylinder is a differentiable simple closed curve and that the initial velocity of the center of the rolling ball has nonzero horizontal (i.e., cross-sectional) component. Then the trajectories of the rolling motion under a constant force parallel to the axis of the cylinder are bounded.*

Let us explore this fact for  $P \subseteq \mathbb{R}^3$  consisting of the vertical strip  $P$  shown in Figure 10. Let  $E_1, E_2$  be the parallel orthonormal vector fields indicated in the figure and write  $v = v_1E_1 + v_2E_2$ ,  $S = sJ$ ,  $J = E_1 \wedge E_2$ . Note that  $E_1$  and  $E_2$  are principal directions with respective principal curvatures  $\kappa(x)$  and 0, where  $\kappa = 0$  on the front and back flat

strips of  $\mathcal{N}_r$  and  $\kappa = -1/r$  on the two half-cylinders. The acceleration due to gravity is the constant  $g$ . Equations (11) reduce to the system

$$\begin{aligned}\dot{v}_1 &= 0 \\ \dot{v}_2 &= -\eta v_1 \kappa(x(t)) s - g \\ \dot{s} &= \eta v_1 \kappa(x(t)) v_2.\end{aligned}$$

Let us set  $v_1 = \text{constant} = u$ . The motion of the center of the ball (in  $\mathcal{N}_r$ ) projects to the cross-section in  $\mathbb{R}^2$  to uniform motion, with speed  $u$ , along the stadium shaped curve  $t \mapsto (x_1(t), x_2(t))$ . Due to translation symmetry, the principal curvature  $\kappa$  only depends on  $(x_1, x_2)$ . We write  $k(t) := \kappa(x_1(t), x_2(t))$ .

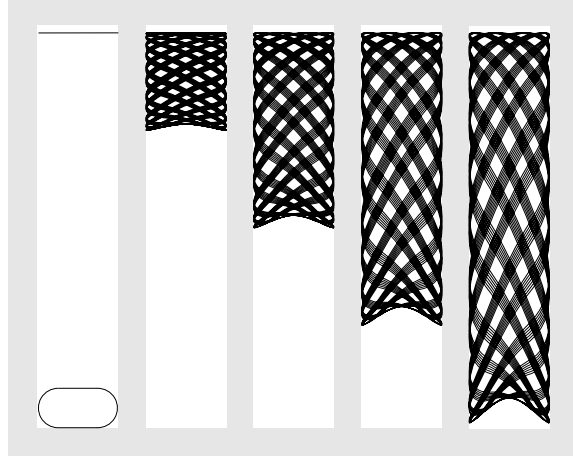


Figure 11: Rolling on a vertical strip under gravity;  $\mathcal{N}_r$  is a cylinder with a stadium shaped cross-section (see bottom-left here, or Figure 10), with  $L = 1$  and  $r = 0.5$ . Acceleration  $g$  increases from left to right ( $g = 0$  on the far left). These trajectories should be compared with those of the no-slip billiard system of Figure 1, illustrating the idea of nonholonomic billiards as smooth approximations of the no-slip kind. (No attempt was made to match parameters.)

Thus we are left to solve the time-dependent system

$$\dot{v}_2 = -\eta u k(t) s - g, \quad \dot{s} = \eta u k(t) v_2.$$

This may be written in matrix form as

$$\frac{d}{dt} \begin{pmatrix} v_2 \\ s \end{pmatrix} = \eta u k(t) \begin{pmatrix} 0 & -1 \\ 1 & 0 \end{pmatrix} \begin{pmatrix} v_2 \\ s \end{pmatrix} - g \begin{pmatrix} 1 \\ 0 \end{pmatrix}$$

This is easily solved by elementary methods. Let  $J$  be the 2-by-2 matrix on the right-hand side of this equation and define

$$N(t) := \eta u \int_0^t k(s) ds, \quad I(t) := \exp \{-N(t)J\}.$$

Then the solution vector  $X(t) = (v_2(t), s(t))^\top$  satisfies

$$X(t) = I(t)^{-1}X(0) - I(t)^{-1} \int_0^t I(s)G ds,$$

where  $G = g(1,0)^\top$ . Solution curves for the center of the rolling ball are shown in Figure 11. Here we see that boundedness of trajectories follows from the general result of Theorem 10. Passing to the limit as  $r$  approaches zero, we recover boundedness of trajectories of the no-slip billiard system on the vertical strip. (Figure 10.)

This example serves as a simple model for higher dimensional cylinders and provides some justification for our proposal of using rolling systems in one extra dimension to illuminate the dynamics of no-slip billiards. The 3-dimensional case, requiring rolling in dimension 4, is naturally more challenging. The remainder of this paper indicates the first steps in this direction.

## 5 ROLLING OVER 3-DIMENSIONAL CYLINDERS IN $\mathbb{R}^4$

In this section we prepare the groundwork for a study of a 4-dimensional ball rolling on a 3-dimensional solid cylinder  $P$  in  $\mathbb{R}^3$ . The immediate goal is to obtain the system of differential equations governing the motion. Those equations will have a hierarchical structure. The rolling hypersurface  $\mathcal{N}_r$  is a product  $\mathcal{N}_r \times \mathbb{R}$  where the cross-section  $\mathcal{N}_r$  is what we call a *pancake surface* in  $\mathbb{R}^3$ . The projection of the rolling motion on this surface satisfies equations that do not depend on the axial variable (height); the cross-sectional trajectories then feed into a set of differential equations for the height function. It was seen above that, for the rolling on a vertical strip in dimension 3, the cross-sectional motion was very simple—uniform motion on a closed simple curve—while the motion on pancake surfaces can be much richer dynamically, as we will see shortly.

### 5.1 SOME GEOMETRIC DEFINITIONS

A few definitions are needed first. Whenever convenient, we regard  $\mathbf{x} = (x_1, x_2) \in \mathbb{R}^2$  as a point in  $\mathbb{R}^3$  or  $\mathbb{R}^4$  by the identification

$$\mathbb{R}^2 = \{(x_1, x_2, 0, 0)\} \subseteq \mathbb{R}^3 = \{(\mathbf{x}, x_3, 0)\} \subseteq \mathbb{R}^4.$$

The cylinder  $P$  is defined by its cross-section  $\mathcal{C}$ , a region in  $\mathbb{R}^2$  whose boundary is differentiable, piecewise smooth, and has bounded curvature. (The assumption that this boundary is differentiable can be relaxed so as to include polygonal regions; in this case, we require the wedge at each vertex made of tangent half-lines to be convex.) We do not require the boundary of  $\mathcal{C}$  to be connected; for example, it could be a strip bound by two parallel straight lines. Now set  $P = \mathcal{C} \times \mathbb{R}$ . We may parametrize the boundary of  $\mathcal{C}$  locally by arclength. If  $\gamma(s)$  is such parametrization, then

$$e_2(\gamma(s)) := \gamma'(s), \quad e_1(\gamma(s)) := -J e_2(\gamma(s)).$$

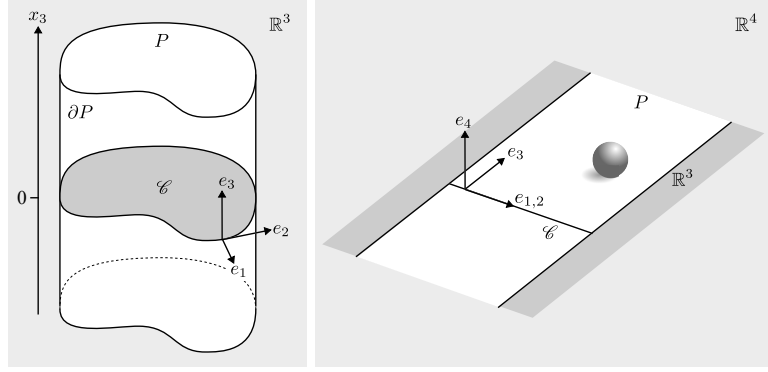


Figure 12: On the left, a general cylinder  $P = \mathcal{C} \times \mathbb{R}$  in  $\mathbb{R}^3$  with cross-section  $\mathcal{C}$ . On the right: schematic picture of the cylinder in  $\mathbb{R}^4$  on which the 4-dimensional ball rolls. The figure shows, in particular, the frame field  $e_1, e_2, e_3, e_4$  adapted to the cross-section contour.

Here,  $J$  is, at each point on the plane, the linear operation that rotates tangent vectors at that point by  $\pi/2$  in the positive direction. See Figure 12 for the orientation used. Further, let  $e_3 = (0, 0, 1, 0)$ ,  $e_4 = (0, 0, 0, 1)$ .

Let

$$P_r = \{x \in \mathbb{R}^4 : \text{dist}(x, P) \leq r\},$$

for  $r > 0$ . For sufficiently small  $r$ , the map  $\pi_P : P_r \rightarrow P$  sending  $x \in P_r$  to its closest point in  $P$  is well-defined and differentiable, and the boundary of  $P_r$ , denoted

$$\mathcal{N} := \mathcal{N}_r := \{x \in \mathbb{R}^4 : |x - \pi_P(x)| = r\},$$

is a differentiable 3-dimensional manifold without boundary. Given  $x = (\mathbf{x}, x_3, x_4) \in P_r$ ,

$$\pi_P(x) = (\mathbf{y}, x_3, 0)$$

and  $\mathbf{y} = \mathbf{x}$  if  $\mathbf{x} \in \mathcal{C}$ , and  $\mathbf{y} \in \partial\mathcal{C}$  if  $\mathbf{x} \notin \mathcal{C}$ . It is also easily seen that  $\pi_P(x + se_3) = \pi_P(x) + se_3$ . Note that the vector fields  $e_1$  and  $e_2$ , initially defined on the boundary of  $\mathcal{C}$ , extend to the complement in  $P_r$  of the interior of  $P$ :

$$e_1(x) := \frac{\mathbf{x} - \mathbf{y}}{|\mathbf{x} - \mathbf{y}|}, \quad e_2(x) = Je_1(x).$$

Thus we have the adapted frame  $e_1, e_2, e_3, e_4$  defined on that extended set.

The hypersurface  $\mathcal{N}$  decomposes as  $\mathcal{N} = \mathcal{N}^+ \cup \mathcal{N}^- \cup \mathcal{N}^c$  where

$$\mathcal{N}^\pm := \{x \in \mathbb{R}^4 : \mathbf{x} \in \mathcal{C} \text{ and } x_4 = \pm r\}, \quad \mathcal{N}^c := \{x \in \mathbb{R}^4 : \mathbf{x} \notin \mathcal{C} \text{ and } |x - \pi_P(x)| = r\}.$$

We refer to  $\mathcal{N}^\pm$  as the *flat parts* of  $\mathcal{N}$  and to  $\mathcal{N}^c$  as the *curved part*. See Figure 13.

The unit normal vector field to  $\mathcal{N}$  is defined at a point  $x$  on the hypersurface by

$$\nu(x) := \begin{cases} \pm e_4 & \text{if } x \in \mathcal{N}^\pm \\ (x - \pi_P(x))/r & \text{if } x \in \mathcal{N}^c. \end{cases}$$

For  $x$  on the curved part  $\mathcal{N}^c$ , define the unit tangent vector  $\tau(x)$  perpendicular to  $e_2$  and  $e_3$ , with the additional property that if  $x \in \mathcal{N}^\pm \cap \mathcal{N}^c$ , then its projection to  $\mathbb{R}^3$  equals  $\pm e_1(x)$ . Note that the  $\nu(x)$  and  $\tau(x)$  and the pair  $e_1(x)$  and (the constant)  $e_4(x)$  both linear span the same plane and the vector fields  $\tau$ ,  $e_2$  and  $e_3$  constitute an orthonormal frame on the tangent bundle of  $\mathcal{N}^c$ . When convenient, we use the more uniform notation  $X_1 = \tau$ ,  $X_2 = e_2$ ,  $X_3 = e_3$ .

We call an  $x_3$ -slice of  $\mathcal{N}_r$  a *pancake surface*. The 0-slice is  $\overline{\mathcal{N}}_r$  and  $\mathcal{N}_r = \overline{\mathcal{N}}_r \times \mathbb{R}$ . Figure 14 shows, on the right, the pancake surface associated to a cylinder  $P$  whose cross-section is a Sinai billiard table. This is a torus with an open disc removed.

## 5.2 A PARAMETRIZATION OF $\mathcal{N}^c$

Let  $\varphi$  be the angle shown in Figure 13,  $0 \leq \varphi \leq \pi$ . Then

$$\nu(x) = \sin(\varphi)e_1(x) + \cos(\varphi)e_4, \quad \tau(x) = \cos(\varphi)e_1 - \sin(\varphi)e_4.$$

Given a local parametrization  $s \mapsto \gamma(s)$  of the boundary of  $\mathcal{C}$  and  $\varphi$ , we obtain a local parametrization of  $\mathcal{N}^c$  as

$$x = a(s, \varphi, x_3) = \gamma(s) + r [\sin(\varphi)e_1(\gamma(s)) + \cos(\varphi)e_4] + x_3e_3.$$

Let  $\kappa(s)$  be the curvature of  $s \mapsto \gamma(s)$ , defined by the expression

$$\frac{d}{ds}e_1(\gamma(s)) = -\kappa(s)e_2(\gamma(s)).$$

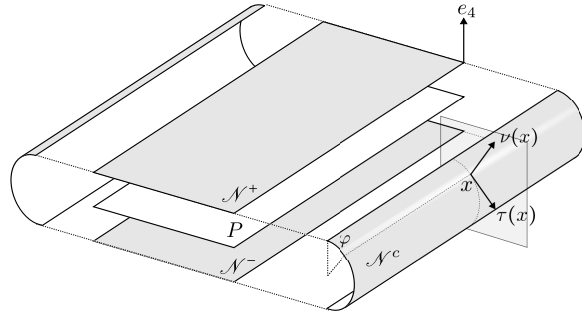


Figure 13: Decomposition of the hypersurface  $\mathcal{N}$  into its flat and curved parts.

For example, if  $\mathcal{C}$  is a disc of radius  $R$ , then  $\kappa = -1/R$ . Relative to this parametrization, the vector fields  $X_1 = \tau$ ,  $X_2 = e_2$  and  $X_3 = e_3$  (expressed as first order differential operators on functions on  $\mathcal{N}$ ) assume the form

$$X_1(s, \varphi, x_3) = \frac{1}{r} \frac{\partial}{\partial \varphi}, \quad X_2(s, \varphi, x_3) = \frac{1}{1 - r\kappa(s) \sin \varphi} \frac{\partial}{\partial s}, \quad X_3(s, \varphi, x_3) = \frac{\partial}{\partial x_3}$$

as is easily shown. Note that  $\kappa(s) \leq 0$  if  $\mathcal{C}$  is convex. The need to make  $r$  sufficiently small in order to avoid focal points in  $\mathcal{N}_r$  is seen clearly in the expression of  $X_2$ . The following proposition, in which  $\nabla$  indicates the Levi-Civita connection on  $\mathcal{N}$  for the Riemannian metric induced from the dot product in  $\mathbb{R}^4$ , summarizes some of the basic properties of these vector fields. Recall that the *shape operator* is defined by

$$\mathbb{S}_x v := -D_v \nu$$

for  $v \in T_x \mathcal{N}^c$ , where  $D$  indicates the Euclidean directional derivative of vector fields.

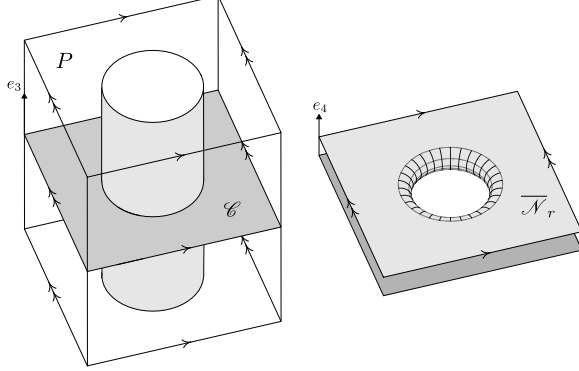


Figure 14: Left:  $P$  is a cylinder whose cross-section is a Sinai billiard table; right: pancake  $x_3$ -slice of  $\mathcal{N}_r$ . Vertical direction:  $e_3$  on the left,  $e_4$  on the right. Compare with Figure 4.

**Proposition 11.** *Define the functions*

$$f_c(s, \varphi) = \frac{\kappa(s) \cos \varphi}{1 - r\kappa(s) \sin \varphi}, \quad f_s(s, \varphi) = \frac{\kappa(s) \sin \varphi}{1 - r\kappa(s) \sin \varphi}.$$

The vector fields  $X_1, X_2, X_3$  satisfy the following properties. Their Lie brackets are

$$[X_1, X_2] = f_c(s, \varphi) X_2, \quad [X_1, X_3] = [X_2, X_3] = 0.$$

Their covariant derivatives are

$$\nabla_{X_2} X_2 = f_c X_1, \quad \nabla_{X_2} X_1 = -f_c(s, \varphi) X_2, \quad \nabla_{X_1} X_j = 0, \quad \nabla_{X_3} X_j = 0, \quad \nabla_{X_j} X_3 = 0$$

for all  $j$ . At each point,  $X_1, X_2, X_3$  are principal directions for the shape operator:

$$\mathbb{S}_x X_1 = -\frac{1}{r} X_1, \quad \mathbb{S}_x X_2 = f_s(s, \varphi) X_2, \quad \mathbb{S}_x X_3 = 0.$$

Finally,  $\nabla_v(X_1 \wedge X_2) = 0$  and

$$\nabla_v(X_1 \wedge X_3) = -\langle X_2, v \rangle f_c(s, \varphi) X_2 \wedge X_3, \quad \nabla_v(X_2 \wedge X_3) = \langle X_2, v \rangle f_c(s, \varphi) X_1 \wedge X_3.$$

*Proof.* These only involve straightforward calculations in Riemannian geometry.  $\square$

### 5.3 THE EQUATIONS OF MOTION ON $\mathcal{N}$

We write the equations of motion (Equations (11) with constant external force) separately on the flat and curved parts of  $\mathcal{N}$ . On the flat parts,  $\mathbb{S} = 0$  and the system decouples into Newton's equation for the motion of the center of the moving ball and constant  $S$  (that is,  $S$  is parallel transported along the trajectory of the center of the ball):

$$\frac{\nabla \dot{x}(t)}{dt} = -ge_3, \quad \frac{\nabla S}{dt} = 0,$$

where ‘.’ indicates derivative in  $t$ . The covariant derivative of  $\dot{x}$  is simply  $\ddot{x}$  on  $\mathcal{N}^\pm$ , so

$$x(t) = x(0) + \dot{x}(0)t - \frac{g}{2}t^2 e_3, \quad S(t) = S(0).$$

Let us focus on the curved part  $\mathcal{N}^c$  and rewrite the equations of motion in the orthonormal frame  $X_1, X_2, X_3$ . Let  $t \mapsto \xi(t) \in \mathcal{M}_{x(t)}$  be a motion of the rolling system, with  $\xi(t) = (S(t), v(t))$ . (See Section 3.3.) The linear and angular velocities are expressed in the orthonormal frame as

$$v(t) = \sum_i v_i(t) X_i(x(t)), \quad S(t) = \frac{1}{2} \sum_{i,j} S_{ji}(t) X_i(x(t)) \wedge X_j(x(t)).$$

Using the properties of the frame fields summarized in Proposition 11, we obtain the derivatives:

$$\frac{\nabla v}{dt} = \sum_i \dot{v}_i X_i + f_c v_2 (v_2 X_1 - v_1 X_2), \quad \frac{\nabla S}{dt} = \frac{1}{2} \sum_{i,j} \dot{S}_{ji} X_i \wedge X_j + v_2 f_c (S_{32} X_1 - S_{31} X_2) \wedge X_3.$$

In addition,

$$S\mathbb{S}v = S_{12} \left( v_2 f_s X_1 + \frac{v_1}{r} X_2 \right) + \left( \frac{v_1}{r} S_{13} - v_2 f_s S_{23} \right) X_3$$

and

$$(\mathbb{S}v) \wedge v = -v_1 v_2 \left( f_s + \frac{1}{r} \right) X_1 \wedge X_2 - v_3 \left( \frac{1}{r} v_1 X_1 - v_2 f_s X_2 \right) \wedge X_3.$$

Plugging these expressions into the equations of motion gives the following proposition.

**Proposition 12.** *The rolling equations, on the curved part of  $\mathcal{N}_r$ , expressed in terms of the orthonormal frame  $X_1, X_2, X_3$  become the following system:*

$$\dot{v}_1 = -f_c v_2^2 - \eta f_s v_2 S_{12}, \quad \dot{v}_2 = f_c v_1 v_2 - \frac{\eta}{r} v_1 S_{12}, \quad \dot{S}_{12} = \eta \left( f_s + \frac{1}{r} \right) v_1 v_2$$

and

$$\dot{v}_3 = \eta \left( f_s v_2 S_{23} - \frac{1}{r} v_1 S_{13} \right) - g, \quad \dot{S}_{13} = -f_c v_2 S_{23} + \frac{\eta}{r} v_1 v_3, \quad \dot{S}_{23} = f_c v_2 S_{13} - \eta f_s v_2 v_3.$$

(Note the separation into equations that contain the subindex 3 and those that do not.)

It is worth noting the hierarchical structure of the equations of Proposition (12): the first set of equations involving  $v_1, v_2, S_{12}$  are independent of  $v_3, S_{13}, S_{23}$  and  $x_3$ . It represents the motion projected to a cross-section. So the full set of equations can be approached by first solving that first set, then feeding the resulting solutions into the second set, which now becomes a time-dependent system. We will explore this observation in greater detail in the next section. For now, further note that the kinetic energy of the system is

$$E = \frac{m}{2} (v_1^2 + v_2^2 + v_3^2 + S_{12}^2 + S_{13}^2 + S_{23}^2) = E_1 + E_2$$

where

$$E_1 = \frac{m}{2} (v_1^2 + v_2^2 + S_{12}^2), \quad E_2 = \frac{m}{2} (v_3^2 + S_{13}^2 + S_{23}^2)$$

and

$$\frac{dE_1}{dt} = 0, \quad \frac{dE_2}{dt} = -mgv_3.$$

Thus the transversal motion is conservative by itself, while  $E_2 + mgx_3$  is conserved, where  $mgx_3$  is the gravitational potential energy. The above proposition should be compared with Theorem 1 about no-slip billiard systems.

#### 5.4 ROLLING FLOWS ON PANCAKE SURFACES

It follows from Proposition 12 that the motion on  $\mathcal{N}_r = \overline{\mathcal{N}}_r$  decomposes into the transversal, free rolling motion on the pancake surface  $\overline{\mathcal{N}}_r$  (see Figure 14) and longitudinal motion governed by the second set of equations in that proposition. Thus the transversal motion is entirely equivalent to the rolling of a 3-dimensional ball on the cross-sectional plate  $\mathcal{C}$ , the 3-dimensional ball having the same moment of inertia parameter  $\eta$  as the 4-dimensional one.

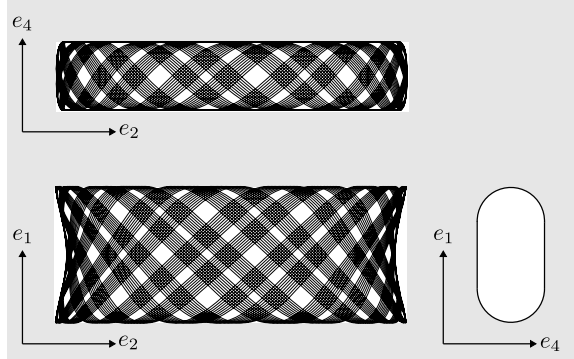


Figure 15: Transversal trajectory in  $\overline{\mathcal{N}}_r$  of the center of rolling ball on the pancake surface for  $P$  bounded by two parallel planes. The cross-section of  $\overline{\mathcal{N}}_r$  (contained in the plane spanned by  $e_4$  and  $e_1$ ) is stadium-shaped (see bottom-left of Figure 11). The longitudinal direction is  $e_2$ .

Let us illustrate this idea with the example for which  $P$  is the region bounded by a pair of parallel vertical planes in  $\mathbb{R}^3$ . In this case, the pancake surface is essentially the same as the cylinder with a stadium-shaped cross-section shown in Figure 10, except that the direction perpendicular to  $E_1$  and  $E_2$  in the figure corresponds to the coordinate vector  $e_4$  in  $\mathbb{R}^4$ .

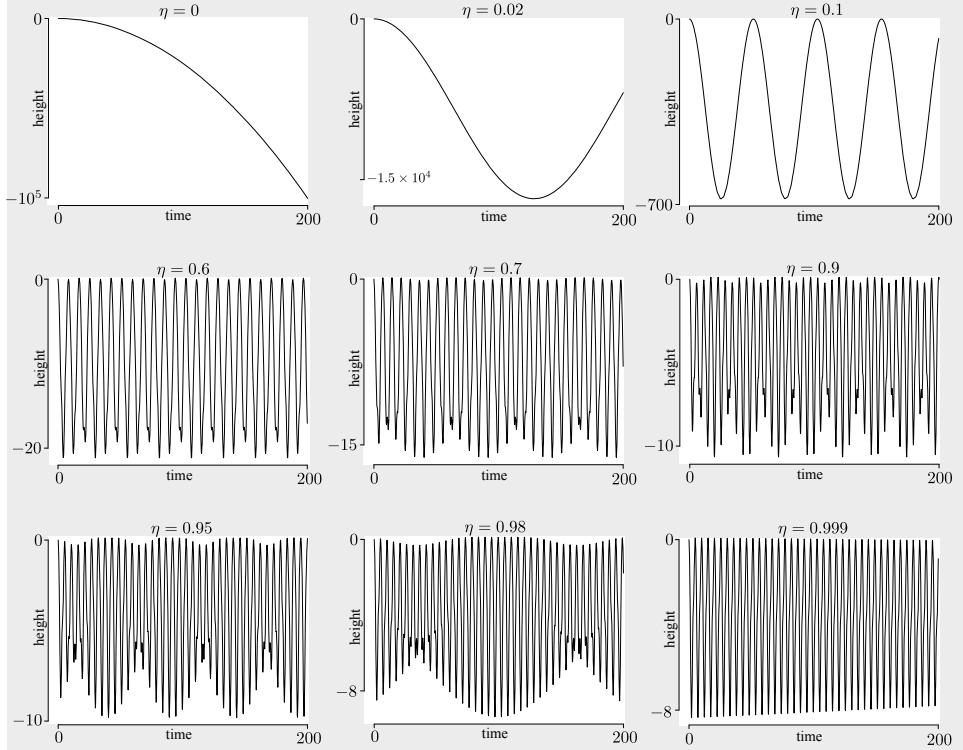


Figure 16: Height function of time ( $x_3(t)$ ) for the nonholonomic billiard on  $P$  consisting of the region between two vertical planes in  $\mathbb{R}^3$  subject to gravity acceleration. When the moment of inertia parameter  $\eta$  is zero (top left), the 4-dimensional rolling ball shows the characteristic parabolic free fall curve. For any positive value of  $\eta$ , initial free fall eventually rebounds and the motion becomes periodic. (For  $\eta = 0.999$ , the periodicity is not apparent in the time range of the above plots.)

Before writing the equations of motion for this example, define on  $\mathcal{N}_r$  the function

$$\zeta(x) = \begin{cases} \frac{\eta v_1}{r} & \text{for } x \in \mathcal{N}_r^c \\ 0 & \text{for } x \in \mathcal{N}_r^\pm. \end{cases}$$

Note that this function is invariant under translation in the  $x_3$ -direction, so  $\zeta(x) = \zeta(\bar{x})$ , where  $\bar{x}$  is the projection of  $x$  to  $\mathcal{N}_r$ . Additionally, this definition anticipates that  $v_1$  is

a constant of motion. Then

$$\dot{v}_1 = 0, \quad \dot{v}_2 = -\zeta(x)S_{12}, \quad \dot{S}_{12} = \zeta(x)v_2$$

are the equations for the transversal motion and

$$\dot{v}_3 = -\zeta(x)S_{13} - g, \quad \dot{S}_{13} = \zeta(x)v_3, \quad \dot{S}_{23} = 0$$

are the equations for the longitudinal motion. These equations are solved just as was done in the example in Section 4.1. Boundedness of the height function ( $x_3$ ), for this example, can be shown analytically as in the case of dimension 3, by the argument used in [4], Proposition 9.

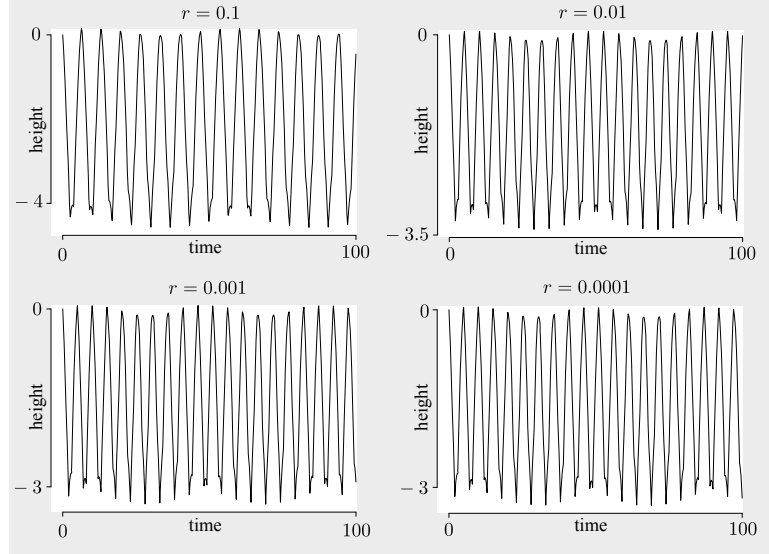


Figure 17: The nonholonomic billiard system converges to a no-slip billiard system as the radius of the rolling ball tends to 0.

**Theorem 13.** *The nonholonomic billiard in the region  $P$  bounded by two vertical planes in  $\mathbb{R}^3$ , under constant acceleration due to gravity, nonzero initial velocity component  $v_1$  (ensuring that the ball will reach the boundary of  $P$ ), and positive moment of inertia parameter, has a periodic (hence bounded) height function.*

Let us see the effect that the moment of inertia parameter has on the height function  $x_3(t)$ . (Figure 16.) For the graphs of Figure 16 we chose  $L = 1, r = 0.5, g = 5, v_1(0) = 1, v_3(0) = -1$  (ball initially rolling from the right to the left vertical plate),  $S_{13} = -0.5$ . (These values are mostly arbitrary, but the corresponding height functions are representative of what is observed generally.) The moment of inertia parameter  $\eta$  must lie in the interval  $[0, 1)$ . For a ball of dimension  $n$ , if all the mass is uniformly

distributed on a thin shell at the surface,  $\eta = \sqrt{2/(2+n)}$  which, in dimension  $n = 4$ , is approximately 0.577. Larger values still make sense if we imagine mass distribution extending beyond the distance  $r$  from the center of the ball to the plate  $P$  on which it rolls, as in a yo-yo.

Figure 17 shows similar graphs to those in Figure 16, for the parameters  $L = 1$ ,  $\eta = 0.39$ ,  $g = 1$ ,  $v_3(0) = -1$ ,  $v_1(0) = 1$ , and decreasing values of  $r$ . This is numerical evidence that the height function stabilizes. The limit value as the radius tends to zero is the no-slip billiard limit.

## 5.5 REMARKS ABOUT THE CIRCULAR CYLINDER

A detailed study of the nonholonomic billiard system on the circular cylinder in dimension 4, which it is hoped will illuminate the observations made about the no-slip billiard system in the 3-dimensional cylinder under gravity, will be undertaken in a future study. This is more subtle than the above system consisting of two parallel planes in that boundedness of orbits for the no-slip system is observed for certain initial conditions but not all. Due to the curvature of the boundary curve of  $\mathcal{C}$  (see the beginning of Section 5 for the definition), the rolling-around-the-edge dynamic cannot be expressed in an explicit analytic form as for the two parallel planes example. In fact, it is not easy to determine a priori for which velocities at a point on the boundary of  $\mathcal{N}_r^c$ , about to enter into this curved part will finally exit it into  $\mathcal{N}_r^+$  or  $\mathcal{N}_r^-$ . (Rolling back into the same flat side from which it entered  $\mathcal{N}_r^c$  is similar to the “friendly roll” phenomenon of a basketball rolling around the rim before falling in or out.) Figure 18 gives some idea of this dynamic.

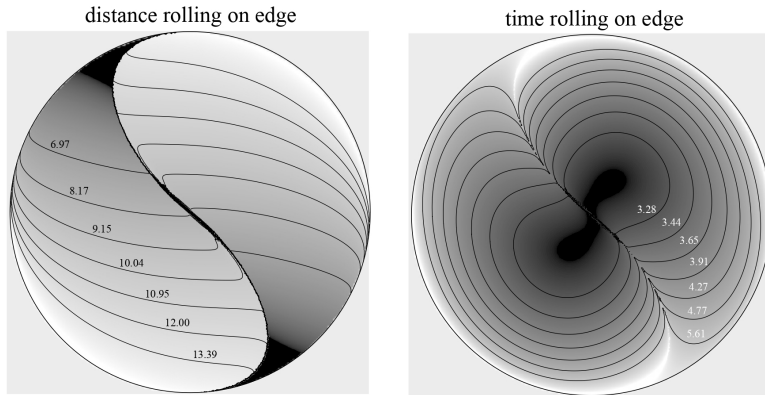


Figure 18: Time spent rolling on the circular edge (right) and distance from the initial point along the edge before reentry in the flat part of  $\mathcal{N}_r$ , shown as a function of the initial velocities. The vertical axis indicates the tangential spin variable  $s$  (component of scaled angular velocity whose axis is perpendicular to the  $x_3$ -slice of  $\mathcal{N}_r$ ) at the moment of crossing from flat to curved part; the horizontal axis indicates the component of the velocity of the center of the ball tangential to the boundary of the flat part. The other component of the center velocity is obtained from this and  $s$  from energy conservation. (Here we used  $r = R$ .)

In order to make sense of these images, recall that the linear and velocities on an  $x_3$ -slice of  $\mathcal{N}_r$  define a vector in a sphere of radius  $\sqrt{2E_1/m}$  where  $E_1$  is the constant kinetic energy of the cross-section subsystem. (See the remark following Proposition 12.) This three-velocity at the moment of crossing the separation circle between flat and curved parts of the cross-section of  $\mathcal{N}_r$  lies in a hemisphere whose pole points into the curved part. The two discs of Figure 18 are the flattening of this hemisphere. The functions represented by their level curves are, on the right, the time spent at the curved part before reentering the flat part and, on the left, the distance around the rim of  $\mathcal{C}$  between the places of entry into  $\mathcal{N}_r^c$  and exit from it.

Despite these complications, we can see, numerically, that the nonholonomic billiard system indeed approximates, for small  $r$ , the corresponding no-slip system. Figure 19 shows a 2-dimensional slice of  $\mathcal{N}_r$  and a segment of trajectory on it. (The dashed circular line shows the boundary between the flat and curved parts of the surface projected flat on the plane.) When the ball's radius tends to zero, the curve approximates the trajectory of a no-slip billiard system, with the characteristic double caustic.

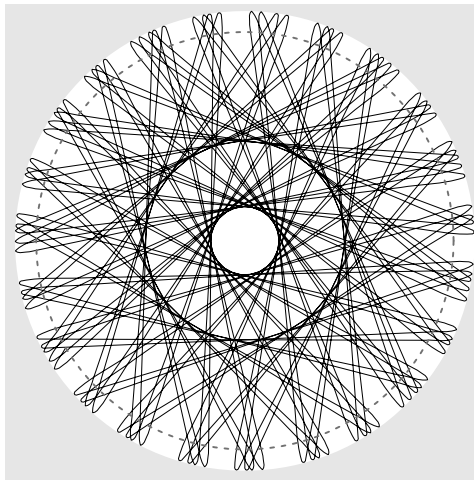


Figure 19: A trajectory of the nonholonomic billiard ball of radius  $r = 0.1$  on a solid 3-dimensional cylinder in  $\mathbb{R}^4$ , whose 2-dimensional cross section is a disc of radius 1. Shown is (the two-dimensional projection of) a 3-dimensional  $x_3$ -slice of  $\mathcal{N}_r$  (a circular pancake surface). The characteristic double-caustic of the no-slip billiard system in a disc is apparent, but instead of a sharp collision at the boundary we see the smooth rolling-around-the-corner reflection.

As for the no-slip billiard system of Figure 2, the height function  $x_3(t)$  of the nonholonomic billiard on the solid cylinder (with a 4-dimensional ball) will typically accelerate downward in an oscillating fashion, but also admits for certain initial conditions bounded motion, as Figure 20 seems to illustrate. (In that figure, the system's parameters are  $R = 1$ ,  $r = 0.1$ ,  $g = 1$ ,  $v_{\text{initial}} = (-0.2, 1, 0, 0)$  for the top example,  $v_{\text{initial}} = (-2, 1, 0, 0)$  for the bottom example,  $S_{21} = -0.61$ ,  $S_{31} = 0$ ,  $S_{32} = 1$ .) The condition of rolling first impact, which we know to be sufficient for bounded trajectories, does not have admit

an obvious counterpart for the nonholonomic billiard system. However, the numerical experiments suggest that, in both cases, boundedness of trajectories is implied by the geometric feature that the two caustic circles typically exhibited by the two-dimensional  $(x_1 x_2)$  projection collapse to a single one.

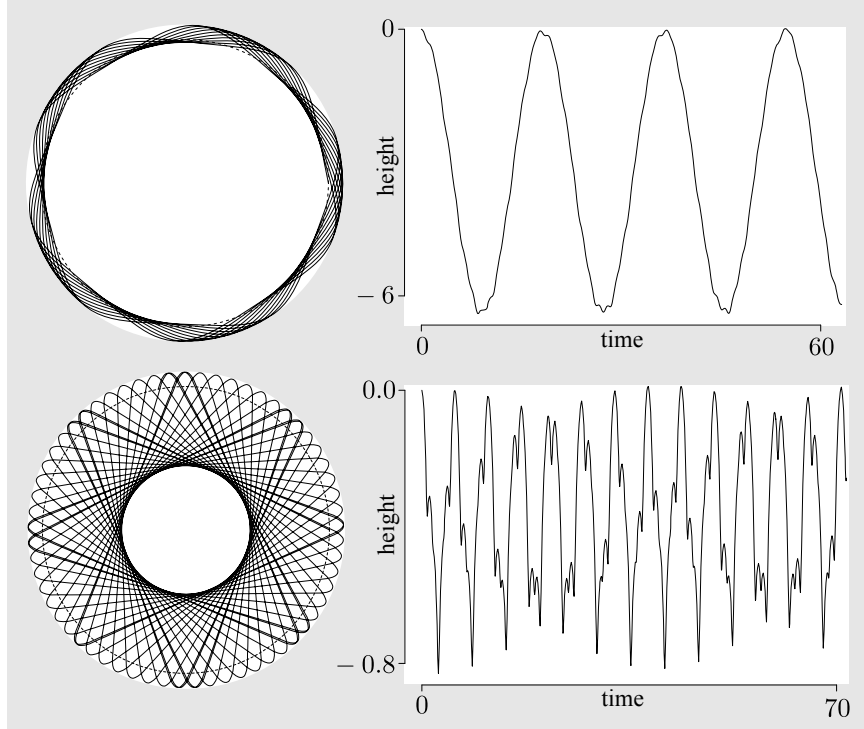


Figure 20: Segments of trajectory (top: with short intervals over the flat part of  $\mathcal{N}_r$ , i.e., skipping motion) for  $r = 0.1$ . Initial conditions were chosen to produce apparent bounded motion, similar to the behavior observed in Figure 2 under the rolling first impact assumption. However, like for the no-slip billiard systems in a solid cylinder, the typical initial condition shows oscillation superimposed to falling. We observe that bounded motion appears in the numerical examples to coincide with the collapse of the two caustic circles into one.

These remarks and numerical work go a certain distance in validating the proposal of this paper that the nonholonomic billiard system can help to illuminate the behavior of the corresponding no-slip billiard system in one dimension lower, but the analytic elaboration of this idea will require further study.

## REFERENCES

- [1] A. V. Borisov, A. A. Kilin, and I. S. Mamaev, *On the Model of Non-holonomic Billiard*, Regul. Chaotic Dyn., **6** (2011), 653-662.
- [2] D. S. Broomhead and E. Gutkin, The dynamics of billiards with no-slip collisions, *Phys. D*, **67** (1993), 188–197.
- [3] C. Cox, R. Feres, B. Zhao. *Rolling systems and their billiard limits*, Regular and Chaotic Dynamics, 2021, Vol. 26, Issue 1, pages 1-21.
- [4] T. Chumley, S. Cook, C. Cox, R. Feres. *Rolling and no-slip bouncing in cylinders*, Journal of Geometric Mechanics, 12(1) 2020, 53-84.
- [5] C. Cox and R. Feres, No-slip billiards in dimension two, in *Dynamical systems, ergodic theory, and probability: in memory of Kolya Chernov*, vol. 698 of Contemp. Math., Amer. Math. Soc., Providence, RI, 2017, 91–110.
- [6] C. Cox, R. Feres and H.-K. Zhang, Stability of periodic orbits in no-slip billiards, *Nonlinearity*, **31** (2018), 4443–4471.
- [7] C. Cox and R. Feres, Differential geometry of rigid bodies collisions and non-standard billiards, *Discrete Contin. Dyn. Syst.*, **36** (2016), 6065–6099.
- [8] R. L. Garwin, Kinematics of an ultraelastic rough ball, *American Journal of Physics*, **37** (1969), 88–92.
- [9] M. Gualtieri, T. Tokieda, L. Advis-Gaete, B. Carry, E. Reffet and C. Guthmann, Golfer’s dilemma, *American Journal of Physics*, **74** (2006), 497–501.
- [10] Brian T. Hefner, The kinematics of a superball bouncing between two vertical surfaces, *American Journal of Physics*, **72**(7):875-883, (2006), 497–501.
- [11] C. Mejía-Monasterio, H. Larralde and F. Leyvraz, Coupled normal heat and matter transport in a simple model system, *Phys. Rev. Lett.*, **86** (2001), 5417–5420.
- [12] M. P. Wojtkowski, The system of two spinning disks in the torus, *Phys. D*, **71** (1994), 430–439.